Ethiopian Institute of Technology – Mekelle

School of Mechanical And Industrial Engineering

A Thesis Submitted To Solid Mechanics And Design Chair In Partial Fulfillment of The Requirements For The Masters of Science Degree In Product Design And Development

Design and Optimization of a Hybrid Polyester Composite for Bus Roof Plates Using Jute and Reused PET Fiber Reinforcement

Ms. Natnael abera

Under the Supervision of

Dr. Abrha G/gergs

Jan, 2025

Mekelle, Ethiopia

THESIS ACCEPTANCE APPROVAL FORM

"This is to certify that the thesis prepared by **Mr. Natnael Abera Gesese**, entitled '***Design and Optimization of a Hybrid Polyester Composite for Bus Roof Plates Using Jute and Reused PET Fiber Reinforcement,'*** has been accepted for the award of the Degree of Master of Science in Mechanical Engineering (Product Design and Development), in partial fulfillment of the requirements for the Master of Science in Mechanical Engineering at Mekelle University."

Members of the Examination Board

Dr. Kalayu Mekonen		19/05/2025
External Examiner	Signature	Date
Dr Alula Gebresas		19/05/2025
Internal Examiner	Signature	Date
Dr Abrha Gebregergs		19/05/2025
Supervisor	Signature	Date
Mr Tadesse Gebray		19/05/25
Chairman	Signature	Date

Confirmation: SMD Chair

ታደሰ ገብረኣይ ተስፋይ (MS c)
የሶሊድ መካኒክስና ዲዛይን ቤይር ሓላፊ
Tadesse Gebray Tesfay (MS.c)
Head of Solid Mechanics & Design Chair

Chair Head	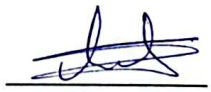	19/05/25
	Signature	Date

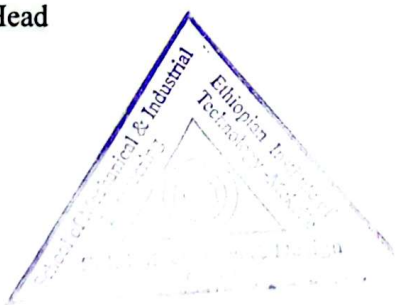

DECLARATION

I hereby declare that this thesis, entitled **"Design and Optimization of a Hybrid Polyester Composite for Bus Roof Plates Using Jute and Reused PET Fiber Reinforcement,"** was prepared under the guidance of my advisor. The work presented herein is my own, except where explicitly stated otherwise. Where I have quoted from the work of others, the source is duly acknowledged. Apart from such quotations, this thesis is entirely my work, and I have declared all significant sources of assistance.

Name of the Candidate: **Mr. Natnael Abera Gesese**

Email address: natnaelabera22@gmail.com

Signature: _____ Date: _____

ABSTRACT

The automotive sector faces rising fuel consumption and pollution due to the increasing vehicle numbers. To mitigate these challenges, lightweight materials have become imperative to diminish the weight of automotive components. Additionally, addressing the pervasive issue of plastic pollution necessitates innovative solutions, such as recycling or reusing the primary plastic pollutant, polyethylene terephthalate (PET). This study tackles two interconnected issues: reducing vehicular weight through material substitution and mitigating plastic waste by reusing PET from discarded water bottles. The main objective of this study is to design and optimise a hybrid polyester composite material for bus roof plates for the modified ISUZU NPR71 4570cc, utilizing jute and reused PET fibers as reinforcement. Samples were prepared using the hand lay-up method, with fiber-to-matrix weight fractions ranging from 40% to 60%. Five laminates were created, incorporating alkali-treated jute fibers to enhance interfacial adhesion. Through a series of experimental tests, the tensile, compressive, flexural, impact strengths, density, and water absorption rates were conducted. The TOPSIS method was applied to assess and evaluate the properties of prepared laminate samples. Results indicate that the P-J-J-P orientation of NaOH-treated jute fiber stands out as the optimal choice. The NaOH-treated jute fiber reduces water absorption by 47% (1.13% compared to 2.13% for untreated jute). A hybrid composite with a P-J-J-P layup and a 0°-90°-0° orientation was used to design a bus roof plate, optimised using HyperWorks-Optistruct and validated through re-analysis with ABAQUS. The optimised jute/PET hybrid polyester composite roof plate achieved a 34.58% weight reduction compared to a mild steel plate, decreasing from 210.38 kg to 137.63 kg, and saved 0.2765 litres of fuel per 100 km. This demonstrates that jute/PET hybrid polyester composites can effectively replace steel structures, offering significant environmental benefits and fuel savings without compromising performance or vehicle load capacity.

Keywords: Reusing PET fibers, Bus roof plate, Modified ISUZU NPR71 4570cc, Lightweight materials, Hyperworks-Optistruct, ABAQUS validation

ACKNOWLEDGMENTS

First and foremost, I would like to express my gratitude to Almighty God for His protection and blessings over the past two years during the difficult time of the Tigray War. I am deeply thankful for His guidance in allowing me to work in a positive environment, surrounded by supportive and knowledgeable individuals, which made it possible for me to complete this research

I sincerely thank my advisor, Dr. Abrha G/gergs, for his invaluable guidance and support throughout my work. His suggestions, advice, and unwavering encouragement were crucial to finish this research. I am particularly grateful for the time he Dedicated to reviewing my work repeatedly and providing valuable feedback. I deeply respect and appreciate his dedication, and I would like to take this opportunity to convey my heartfelt thanks.

I am grateful to the School of Mechanical and Industrial Engineering, and the School of Civil Engineering at the Ethiopian Institute of Technology, Mekelle (EIT-M), Mekelle University, for providing the laboratory materials and services that supported my research.

Furthermore, I would like to express my heartfelt gratitude to my friends and colleagues, Mr Dejene Grima and Ms Fikrte Gebrezgabihar, for their kind support during the preparation and testing of the composite laminate samples, and throughout the entire research process. Words cannot fully express my appreciation.

Finally, I would like to thank my family for their unwavering support and encouragement throughout my years of study and during the writing of this thesis. And A special thanks to my little brother, Eul Abera, who is truly special to me. I can never repay you for all you've done. This accomplishment would not have been possible without you.

Thank you very much.

TABLE OF CONTENTS

LIST OF ABBREVIATIONS AND ACRONYMS

[A]	Membrane stiffness of a laminate;
[B]	Bending-extension coupling stiffness of a laminate
[D]	Bending stiffness of a laminate;
[Q]	Reduced material stiffness matrix
ASTM	American Society for Testing and Materials
BCs	Boundary constraints
CLT	Classical Laminate Theory
CPT	Classical Plate Theory
E_1, E_2	Lamina longitudinal and transverse moduli composite
F	Force (N)
FEA	Finite Element Analysis
G_{12}	In-plane shear modulus
Mpa, GPa	Megapascal, Gigapascal
J	Jute
σ_b	Bending stiffness
Mx, My	Bending moments per unit length at the mid-surface of a plate
Nx, Ny, Nyx	Membrane forces per unit length at the mid-surface of a plate
PET	Polyethylene terephthalate
V_f, V_m	Fibers and matrix volume fraction
V_{12}	In-plane Poisson's ratio
x_t, x_c	Tensile and compression strength in the fiber direction
y_t, y_c	Tensile and compression strength in the transverse direction
TOPSIS	Technique for Ordering Preference by Similarity to Ideal Solution
θ	The angle between the global x-axis and the material direction local axis
ρ_f, ρ_m	Density of Fiber and matrix (g/cm^3).
σ	Tensile stress (MPa).
σ_1, σ_2	Normal stress in plane 1 and 2
τ_{12}	Shear stress in 1-2 plane

LIST OF TABLE

LIST OF FIGURES

CHAPTER ONE

1. INTRODUCTION

1.1. Background

There is increasing concern about fuel consumption and pollution due to the rising number of vehicles. The automotive industry faces significant pressure to lower fuel usage and emissions [1]. Approximately 75% of a vehicle's fuel consumption is influenced by its weight. Directly reducing weight by using lighter materials is crucial for the industry. One potential solution to these issues is reducing the weight of individual car components. As a result, composite material is recently used widely in aerospace and automotive industries, one is continuously looking for ways to lower the overall mass of the aircraft and vehicle without decreasing the strength and stiffness of its components [2], [3]. Developing lighter materials is a key strategy to address the economic benefits of using easily available materials while avoiding the drawbacks of heavy components in vehicles [4]. Composite materials play a significant role as engineering materials, and their use has Rising due to their high strength-to-weight ratio, high modulus-to-weight ratio, corrosion resistance, and wear resistance [5]. Most automotive manufacturers use natural fibers composite in their products aiming to minimise the cost, vehicle weight, life cycle, and environmental impact [4], [5].

On the other hand, the excessive use and improper disposal of plastic water bottles are influential to pollution, biodiversity loss, habitat destruction, and climate change [6]. Once discarded, these bottles can persist in the environment for centuries, adding to the problem of plastic pollution. Despite their environmental drawbacks, plastic has better durability, strength, and flexibility making it a popular material in various industries and sectors. This widespread use has led to significant environmental pollution that impacts our daily lives. However, there are solutions to mitigate plastic pollution, such as using biodegradable and compostable materials, reusing plastic items, and recycling. Implementing these strategies can reduce the negative effects of plastic on our planet [7], [8].

To tackle these issues, a crucial solution involves minimizing environmental pollution and fuel consumption in a vehicle by reusing the primary plastic pollutant, polyethylene terephthalate, in combination with natural fibers. The hybridization of natural fibers such as jute, sisal, rice straw,

flax, banana fiber, hemp, and sugarcane with synthetic fibers like PET (polyethylene terephthalate), e-glass, and acrylics can greatly improve the performance of polymer composites, increasing their versatility for various applications. This hybridization method enables the adjustment and enhancement of the composite's properties to meet specific requirements [9]. Among all natural fibers, jute appears to be the most useful, and economical and exhibits moderately higher mechanical properties [4]. The high cellulose content and low micro-fibril angle of jute fiber provide good reinforcement in the polymer matrix and exhibit inherent advantages like low density, high specific strength, and stiffness. Additionally, Jute's natural capacity to absorb vibrations is crucial for automotive applications under impact loading conditions, leading to better ride comfort and lower noise levels [5] and it is fully biodegradable. On the other hand, PET fibers exhibit excellent properties such as good strength, elasticity, heat retention, and resistance to acids, and alkalis [10]. By designing the stacking sequence of laminate, and optimizing the composite structure it is possible to achieve lightweight, high-performance materials suitable for a wide range of applications.

This study explores the potential benefits of using hybrid polymer composites in specific areas of the bus roof plate for the modified ISUZU NPR71 4570cc bus, through experimental characterization, analytical modeling, Optistruct optimization, and Abaqus validation. By combining jute with PET fiber, the properties of the composite are enhanced.

Figure 1-1: Modified ISUZU NPR71 4570cc bus

1.2. Problem Statement

The automotive manufacturing sector is increasingly focused on enhancing weight reduction, performance, and fuel efficiency through the development of alternative materials. Steel, despite its favourable weight-to-strength ratio, remains the primary material in vehicle production, constituting up to 65% of a vehicle's average weight [11]. This reliance poses significant challenges, as steel's weight contributes to higher fuel consumption and CO2 emissions, particularly in vehicles like the modified ISUZU NPR71 4570cc buses, which currently use steel for their roofs, leading to unnecessary weight and fuel inefficiency, despite steel's favourable weight-to-strength ratio. given these challenges, there is a pressing need to investigate hybrid composite materials as a lighter, balanced alternative. This study aims to assess the feasibility of replacing the steel roofs of these buses with hybrid composites, ensuring that they meet the required strength and performance specifications without compromising safety or functionality.

Figure 1-2: Roof of modified ISUZU NPR71 4570cc buses

1.3. The objective of the study

1.3.1. General Objective

The main objective of this study is to design and optimise a hybrid polyester composite material for bus roof plates, utilizing jute and reused PET fibers as reinforcement.

1.3.2. Specific Objectives

The specific objective of this project is;

1. To investigate the physical and mechanical properties of jute/PET fiber through hybridization and alkali treatment of natural fiber.
2. To select the best laminate stacking sequence of jute/PET fiber hybrid reinforced polyester composites using a TOPSIS method.
3. To design and optimize the size of the existing bus roof by jute/PET fiber hybrid reinforced polyester composites using CLT and Altair HyperWorks software (Optistruct)
4. To validate the optimized hybrid bus roof by using FEM (ABAQUS).

1.4. Scope of the Project

The scope of this study is to enhance, investigate, and design a bus roof material from jute/PET fiber hybrid reinforced polyester composite based on the collected related data, and analysis investigated. These researches attain the chemical treatment of the jute fiber, and sample fabrication, characterizing the mechanical and physical properties, testing based on the ASTM standards, selecting the best stacking sequence laminate based on the TOPSIS method, designing a jute/PET fiber hybrid composite, optimizing the geometry of the bus roof using Altair Optistruct, and validate the optimized hybrid composite using Abaqus and analyzing the economic advantages of the designed part. Furthermore, this research targets, a bus roof of modified ISUZU NPR71 4570cc buses.

1.5. Significance of the Study

The significance of this study lies in its potential to reduce fuel consumption and enhance vehicle performance by replacing steel bus roofs with a hybrid composite made from natural fibers and reusing PET fibers. Hence, the hybrid composite material has a high strength-to-weight ratio, corrosion resistance, environmentally sustainability, and wear resistance, making it a viable alternative for automotive manufacturing. By demonstrating the feasibility of locally fabricating these components, the study aims to promote cost-effective, eco-friendly solutions, raise awareness among manufacturers, and encourage the adoption of sustainable materials in the automotive industry.

1.6. Justification of Study

Automotive companies have been working hard to make cars lighter and more fuel-efficient. They've been experimenting with new materials to achieve these goals. Many researchers have studied the weight optimization of vehicle components for economic advantages and resource-utilizing influence on the community [1], [11], [12]. With the increasing awareness of environmental sustainability, composite materials are used because of their sustainable benefits, such as being more economical and biodegradable. Researchers use synthetic fiber as a reinforcement to replace the existing material of automotive components. Using synthetic fibers for the composite material is another cost increase for the material [13]. Using hybridized composite material can be a choice that provides benefits in terms of energy conservation, minimizing production costs, and conservation of material resources. Despite many challenges, developing the use of composite material in the manufacturing of automotive components is a current emerging area of study, especially hybridized fiber material [14]. Thus, hybrid composite material plays a major role in the automotive field due to its mechanical and physical properties to balance the strength-to-weight ratio without sacrificing its strength, performance, and safety.

CHAPTER TWO

2. LITERATURE REVIEW

This chapter reviews and synthesizes relevant studies, previous research, data, and findings to establish and identify existing research gaps. Furthermore, It focuses on earlier investigations of hybrid jute/PET polymer matrix composites, discussing results and characterization standards that acted as benchmarks for this work. The chapter also highlights the essential properties that define these composites, provides an overview of laminate structure analysis, and examines the effects of weight reduction on vehicles.

2.1. Introduction

A composite material system is composed of two or more physically distinct phases whose combination produces aggregate properties that are different from those of its constituents [15]. One component is known as the reinforcing phase, while the surrounding component is called the matrix. The reinforcing phase can be made up of fibers, particles, or flakes, while the matrix is usually continuous. In recent decades, reinforced polymer composites have gained popularity because of their enhanced properties and availability compared to traditional monolithic metals like steel and aluminum. Composites are categorized based on their matrix materials into metal, ceramic, and polymer matrixes. Polymer matrix composites are particularly versatile, finding use in various applications due to their low density, excellent thermal and electrical insulation, and cost-effectiveness [15], [16].

Based on the type of reinforcement, polymer composites are categorized into fiber-reinforced polymer composites and particle-reinforced polymer composites. Fiber-reinforced polymer composites demonstrate outstanding performance and can be easily produced by combining cellulose fiber molecules with resin in the fiber-reinforced matrix. Various factors affect the performance of these composites, including the properties of the fibers, their orientation, fiber content, fiber matrix, and interface. Notably, fiber orientation is a crucial factor in the design of composite materials, as it can significantly impact their performance [15], [17]. Researchers are currently focusing on fiber-reinforced polymer composites, which are increasingly gaining traction in engineering applications [18].

2.2. Study on Polymer Matrix of Composite

The matrix or resins used in fiber-reinforced composites are often referred to as "polymers." All polymers share a key characteristic: they comprise long, chain-like molecules composed of numerous repeating units that define their suitability for various applications. Generally, polymers can be divided into two main categories: thermoplastics and thermosetting polymers. Among the most commonly used thermosetting resins are epoxy and polyester resins. Unsaturated polyester resins also known as general polyesters, fall under this category [5], [19]. Thermoset polymers are materials that harden permanently due to a network of strong chemical bonds between their molecules. Once they've set, they can't be reshaped or softened. Strong bonds between the filler and the polymer are crucial for creating a composite with good mechanical strength [20].

When the resin is heated beyond its glass transition temperature (Tg), there is a notable change in its mechanical properties, which can be reversed by cooling it back below Tg. Above this temperature, stiffness decreases significantly, decreasing the composite's compressive and shear strength [21]. The fabrication and shaping of composite materials into finished products can be done using various methods. One of the most commonly used and simplest techniques is the hand lay-up method, suitable for manufacturing small and large reinforced thermoset products. The hand lay-up open mold technique is a straightforward process for forming and shaping composites [5], [22].

Numerous researchers, [5], [23], [24] have conducted experiments to enhance the mechanical properties of polymer composites that incorporate natural fibers, owing to their attractive features such as flexibility, low cost, availability, biodegradability, and lightweight nature.

2.3. Study on Natural Fiber

The natural fibers used for reinforcement include sisal, jute, rice straw, flax, banana fiber, hemp, and sugarcane fibers. These natural fibers are cultivated as crops [25]. Among these, the best-performing fibers (kenaf, hemp, jute, and flax) demonstrate superior flexural strength and modulus of elasticity, while leaf fibers like sisal exhibit excellent impact properties. Natural fibers are composed of cellulose microfibrils dispersed within an amorphous matrix of lignin and hemicellulose [26], [27].

Figure 2-1: (a). Jute plant, (b). Jute fiber and (c). Meshed Jute [19], [28]

Jute fiber is the finest fiber and is a long, soft shiny fiber that can be spun into a coarse and strong tread. It has good tensile strength and is a good thermal and electrical insulator [19], [28].

Table 2-1: Properties of jute fibers [4], [29], [30], [31], [32], [33]

Properties	**Unit**	**Jute fiber**
Density	g/cm^3	1.3 – 1.5, average 1.4
Tensile strength	kN/mm^2	610 – 780
Stiffness	kN/mm	15 – 35
Elongation at break	%	1.0 – 1.9
Max. elongation	Mm	10 – 14
Tensile modulus	Gpa	12 – 60
Youngs modulus	Gpa	15 – 30
Cellulose content	%	59 – 70
Hemicellulose content	%	15 – 20
Fiber length	Mm	120 – 900
Microfibrillar angle	Deg	8 – 9

Recently, natural fiber-reinforced polymers have created interest in the automotive industry for the following reasons [14], [15], [8]

- They are environment-friendly, meaning that they are biodegradable.
- The density of natural fibers is low compared to glass and carbon fiber, in the range of 1.25 - 1.5 g/cm^3.
- The modulus-weight ratio of some natural fibers is greater than that of E-glass fibers.
- Natural fibers are much less expensive than glass and carbon fibers.

2.3.1. Characterization of Natural Fiber in Hybrid Composites

Natural fiber has a high aspect ratio a high strength-to-weight ratio, is low in energy conversion, and has better insulation properties. The fiber's inherent hydrophilic nature makes it susceptible to water uptake in moist conditions, which directly affects the mechanical properties, such as stiffness and strength, which are negatively influenced and decreased. To overcome this limitation the fiber-matrix adhesion may be improved and the fiber swelling reduced using chemical treatments such as alkaline treatment, silane treatment, benzoylation, peroxide treatment, and permanganate treatment [34], [35]. Alkaline treatment is the cheapest and the most applied of all methods [34].

A research study [36] found that jute natural fiber is an excellent and most important sound-absorbing and (vibration absorbing material) damping characteristics material with greater savings in weight and cost without causing harm to the environment. In the application of automobile roofing, flooring, door panels, and engine partition parts it is eco-friendly, biodegradable, and economical. jute natural fiber is an alternative to noise-controlling materials [37].

The development of jute hybrid composites in car panels [21] studied the stiffness and flexural strength of jute epoxy-reinforced composite for car panels. Steel is much heavier than jute composites. For the area of 118.24mm^2, jute composite weighs 0.4414N and mild steel weighs 3.375N. This means steel-made cars are bulkier, slower, and less fuel-efficient. Jute composites could help improve movement, handling, fuel efficiency, and carbon dioxide emissions.

According to the comparative evaluation of properties of hybrid glass fiber - sisal/jute reinforced epoxy composite research result, the addition of sisal fiber with GFRP exhibited superior properties than the jute fiber with GFRP composites in tensile properties and jute fiber reinforced GFRP composites performed better in flexural properties [38]. The reinforcement of natural fibers with synthetic fibers reduces moisture absorption, improving overall material performance. These hybrid composites are gaining popularity due to their advantages over synthetic fibers. However, while they improve certain properties, their performance still falls short compared to pure GFRP.

The effect of the weight percentage of jute fiber reinforced in polypropylene-based composites found that mechanical properties increased as the jute weight percentage increased up to 40% [39]. In comparison to natural to synthetic fibers, natural fibers have a special advantage in biodegradability and are abundantly available from renewable resources But their properties of

hydrophilic and high moisture content lead to poor interface between the fiber and matrix and to improve the interface in natural fibers, several chemical treatment methods can be used. [20]. The mechanical and water absorption properties are enhanced when the natural fiber is treated. Alkali treatments improve tensile, compression, and impact strengths while reducing water absorption [40]. To accomplish the desired enhanced adhesion between the hydrophilic fibers and the hydrophobic PM Chemical modification is necessary. The alkali treatment of fibers is the most prevalent and effective way for the chemical modification of fibers [41].

2.3.2. Investigation of Chemical Treatment of Natural Fibers in Composite

Natural fibers are chemically treated to remove impurities, lignin, pectin, waxy substances, and natural oils covering the surface of the fiber cell wall. Mercerization is the treatment of natural fibers to have good interfacial bonding between the reinforcing fiber and the risen matrix in the composite. Sodium hydroxide (NaOH) is the most commonly used chemical for treating the surface of plant fiber fine structure of the native cellulose I to cellulose II by a process known as alkalization. NaOH alkali solution treatment of jute enhances the mechanical properties, it gives a rough surface having good mechanical interlocking, increases fiber uniformity, adhesive characteristics of jute fiber surface by removing natural and artificial impurities, increases dispersibility and well separated, increases the tenacity, the modules of jute fiber, and reduction in weight Treatment of natural fiber is important to improve the bonding between the fiber and matrix for composite application to increase tensile strength, tensile modulus and flexural strength of the composite [42], [34], [43].

The effect of chemical treatment on jute fiber in the fabrication of composites, and the study's results show that the alkaline treated specimen improved in impact strength by 20% when compared to the untreated fiber of jute [19]. Regardless of the desirable natural fibers as reinforcement in composite materials have some challenges [44]. This includes incompatibility with hydrophobic matrix and a tendency to form aggregates. Consequently, researchers adopted a method for improving the compatibility of natural fibers with hydrophobic matrix. The alkaline treatment of jute fibers with a 5% aqueous NaOH solution showed a significant change in the mechanical properties of natural fibers reinforced composites [45].

The experiment was conducted on jute fiber with a solution of 5 w% NaOH for 24 hrs. at room temperature, and then after removing the excess NaOH with distilled water found to improve in mechanical properties [46]. Chemical treatment was among the methods that activated the hydroxy chemical group to make fiber compatible with the matrix [47]. The alkali treatment of jute fiber improves the load shearing capability, resulting in higher tensile strength in composites by removing cellulosic materials and making the fiber more capable of rearranging itself along the fiber direction and improving fiber-matrix adhesion [48]. The flexural strength of 5 % alkali-treated jute fiber/unsaturated-polyester resin composites treated for 2h and 4h increased by 3.16% and 9.5%, respectively, when compared to untreated jute fiber composites [49].

The alkaline treatment enhances the bond between jute fibers and the matrix, reducing water absorption and improving impact strength. This treatment improves the mechanical and physical properties of natural fibers by addressing the water-absorbing hemicellulose in jute. As a result, the overall performance of the treated jute fibers is significantly enhanced [50]. Chemical treatments considered in modifying the properties of the natural fibers; including sodium hydroxide, acetic acid, silane, benzoylation, acylation, malleated coupling agents, isocyanates, and potassium permanganate were studied. V.A. The characteristics of jute fibers that were enhanced with alkaline (NaOH) treatment resulted in an increase in tensile strength from 44.3 to 63 MPa (42.2%) and flexural strength was found to increase from 56.2 to 64 MPa (13.9%) [27].

2.4. Study on the impact of disposal of waste plastic bottle

Plastic has become an integral part of modern life, influencing various aspects of our daily activities. The rising demand for plastics and plastic products is a major contributor to environmental pollution. Globally, over 300 million metric tons of plastics are produced each year from more than 20 different types of plastic [51], [52]. In Tigray, over 23 million plastic bottles and bags are consumed annually, with most ending up in the solid waste stream, creating significant challenges for waste management [53]. Despite the many disadvantages, plastics offer considerable benefits, such as being cost-effective, lightweight, and versatile.

The non-biodegradable nature of plastics contributes to severe environmental pollution, impacting soil, water, and air quality. Different studies explore the toxic effects of plastics on human health and the environment, due to harmful chemicals like Bisphenol A (BPA), phthalates, and

brominated flame retardants, especially at high temperatures, which can lead to toxic chemicals leaching into food and water. Furthermore, improper disposal practices and open burning release harmful substances into the air, posing serious health risk issues including respiratory problems, liver dysfunction, skin diseases, and even cancers [6], [7], [8].

Figure 2-2: Waste plastic bottle [54]

Implementing proper regulations around the production and use of plastics could mitigate these toxic effects. As a result, there is a pressing need for effective management strategies, including recycling, reusing, and the development of biodegradable alternatives [8], [52].

Plastic bottles are bottles made of high or low-density plastic, such as polyethylene terephthalate (PET), polyethylene (PE), polypropylene (PP), polycarbonate (PC), or polyvinyl chloride (PVC). Each of the materials mentioned has a distinct function, which includes [55]:

1. PET: a type of plastic used to carry water and refreshments on the go.
2. PE: a stiff plastic bottle material used to make squeeze bottles.
3. PP: a plastic that is used to make pharmaceutical bottles (pills)
4. PC: a material that is used to create refillable and reusable containers.
5. PVC: a durable material used for products that require long-term storage.

2.5. Reviews on the PET and PET fiber hybrid composite

PET: Reacting petroleum hydrocarbons with ethylene glycol and terephthalic acid, to create thermoplastic polymer. The polymer might be opaque or transparent depending on the particular material makeup. Polymerization is used in the production process, which results in long molecular chains that can later be used to build PET bottles. A high concentration of acetaldehyde in PET

used during bottle manufacturing might give the beverage inside an off taste. the PET bottle production stage begins After the plastic has been created [55].

PET (polyethylene terephthalate) is a commonly used plastic material found in numerous single-use items, including water bottles, food containers, and packaging. When improperly disposed of, plastic waste accumulates in landfills and water bodies, where it persists for hundreds of years, releasing harmful chemicals and disrupting fragile ecosystems.

Table 2-2: Properties of PET [10], [56], [57], [58]

Properties	**Unit**	**PET**
Coefficient of friction	-	0.2 - 0.4
Hardness – Rockwell	-	M94 – 101
Izod impact strength	J/m	13 – 35
Poissons ratio	-	0.37 – 0.44
Density	g/cm^3	1.3 – 1.4 Average 1.35
Flammability	-	Self-extinguishing
Tensile strength	kN/mm^2	80, for biax film 190-260
Stiffness	$kN/mm2$	2.8 – 3.5
Elongation at break	%	60 – 165
Tensile modulus	Gpa	2 – 4
Youngs modulus	Gpa	2 – 3.5
water absorption – over 24 hrs	%	0.1

An experiment was conducted [59], to evaluate the effectiveness of recycled waste polypropylene (PP) by comparing waste PP-jute composites with virgin PP-jute composites. The study involved collecting, washing, drying, and mechanically recycling waste PP into granules, and using jute fibers as a reinforcing agent. Composites with varying jute fiber percentages (5 wt.% - 30 wt.%) were produced through injection molding. The results indicated that virgin PP had a 6% higher tensile strength and a 19% greater elongation at break compared to waste PP. and, the performance of waste PP-jute composites was nearly equivalent to that of virgin PP-jute composites and the chemical structures of waste and virgin PP are nearly identical, with no significant degradation of waste PP. Physico-mechanical tests demonstrated similar results for both types of composites suggesting that recycled PP can be both economically and environmentally viable. The potential

for recycled PP to reduce waste while providing composites with good mechanical properties for construction and other industries is significant [60].

The research focuses [61], on characterizing injection molded PET composites reinforced with sisal fibers subjected to different treatments. Composites containing 40 wt.% of untreated, alkaline-treated, and alkali/acetylated sisal fibers were prepared through compounding and injection molding. The insertion of 40 wt.% sisal significantly increased the tensile modulus by 137%, with alkali-treated sisal further enhancing it by 179%, and the combined alkali/acetylation treatment yielded a 233% improvement. These enhancements are crucial, as modulus is a key factor in engineering design and performance. Overall, the mechanical, thermal, and water absorption properties of the alkali-treated and alkali/acetylated sisal composites showed substantial improvements over the raw sisal composite [62]. Compared to commercially available natural fiber-reinforced thermoplastic composites in the automotive industry, the sisal-PET composites demonstrated a remarkable increase in flexural strength (66.6% to 190%) and flexural modulus (110.5% to 410%), depending on the treatment and comparison [61]. Therefore, these composites are recommended for various automotive applications.

Most plastic products should be recycled or reused since they are non-biodegradable and do not easily integrate into the environment. The recycling of PET and the creation of recycled PET (rPET) or polyester composites reinforced with various natural fibers, emphasize their environmental benefits by repurposing them into secondary products, thereby promoting sustainability [63]. PET is a low-cost, high-performance thermosetting polymer widely used in packaging due to its abrasion resistance, hardness, solvent resistance, and stiffness [10]. PET has fascinating physical and chemical properties as a thermoplastic polyester resin. It is a semi-crystalline polymer that behaves like an amorphous glass at lower temperatures. When heated above 72°C, PET transforms from a rigid, glass-like state into a flexible, rubbery form [63].

Jute fiber-reinforced PET and a mixture of PET/ Linear low-density polyethylene (LLDPE) composites (50% fiber by weight) were prepared by compression molding. A fraction of PET and LLDPE was varied from 20-80% by weight in the composites and the mechanical properties were investigated and compared over PET/jute composites [64]. It was found that with the increase of LLDPE in the composites, a fraction of the mechanical properties were decreased due to the

incorporation of the LLDPE except elongation at break (Eb%). LLDPE blended with PET-based composites gained a significant improvement in the Eb (%). Composites lost their mass slowly in soil medium and thus indicated their semi-degradable characteristics.

2.6. Characterization of Water Absorption Property on Hybrid Composite

A research study of water absorption properties of natural fiber-reinforced polyester composite [40] clearly showed that the water absorption rate with pure polyester increases treated fiber and untreated fiber content after 24 hours, and the result showed that the percentage of water absorption is increased with the increasing of fiber content and reduced with the alkali treatment of natural fibers. Pure polyester's water absorption rate reaches 0.4%, untreated 20% sisal fiber is 10%, and treated 30% sisal fiber is 2.8%. This showed that the alkali treatment of natural fiber improves the water absorption rate by creating an outer surface layer resistant to water. Additionally, increasing the fiber content improves the impact property of the composite.

Woven composites and interwoven hybrid composites were tested for the effects of water absorption on tensile and flexural properties compared between the dry and wet samples obtained by immersion of the composite samples into tap water until reaching the saturation point result. The study showed that the water absorption and mechanical properties enhanced through hybridization with interwoven processes than individual woven ones. The strength and modulus properties are reduced with water resistance decreasing or increasing water penetration by matrix cracking, voids, delamination, and a weak bond interface between the matrix and fiber [65].

2.7. Review on the Effects of the Stacking Sequence of Composite Laminate

Fabrication of composites from jute and glass fiber research study [22] investigated the best laminate stacking sequence of the composite. G-J-J-G laminate composite has better mechanical properties, like impact strength and ductility than J-G-G-J laminate. Laminate with stacking sequence G-G-G-G has high tensile strength causing pure brittleness. In addition, the G-J-J-G laminate is used as a structural component in a medium load [66].

The mechanical properties of jute woven fabric composites and their hybrids have been investigated in the research work [67]. Jute woven fabric composites were sandwiched with glass woven composites with the epoxy matrix. The increase in tensile properties of jute composites depends on the number of glass composites hybridized or sandwiched with jute composites. The bending and impact properties will significantly increase by adding thin layers of glass composites as skin or outer layers into jute composites to reduce water absorption. The bending strength and impact of jute–glass sandwich is higher than nearly twice that of jute composites. The use of glass fiber in the composites increases the ductility [68]. The best mechanical properties of composites can be obtained when the fiber is aligned parallel to the direction of the applied load [69]. Several layers and layering sequences on the fibers affect the mechanical properties, like tensile, flexural, and impact strength on the composite material [70]. According to the study, tensile and flexural strength is better when the synthetic fibers are layered at the outer with an increasing number of layers and impact is better when the natural fiber is layered at the outer surface.

Decision-making tool for different alternatives with multiple criteria

Choosing and applying appropriate decision-making methods has a vital role in the simplifying of design optimization of a particular part or feature [71]. One of the decision-making tools for solving problems with multiple criteria of alternatives from the given one is the TOPSIS (Technique for Ordering Preference by Similarity to Ideal Solution) method, which is a multi-criteria decision-making tool that shows the shortest distance from the ideal solution and the longest distance from the negative ideal solution. The positive best alternative maximized the beneficial attribute and the negative best alternative minimized the cost attribute fitted the best solution [72], [73]. It has numerous advantages, easy to use, fast, and relatively simple, and a systematic procedure.

The TOPSIS method is used to solve problems with multiple objective optimization problems in ranking composite materials by considering different variables which help to choose the best alternative from a set of alternatives [74]. TOPSIS solves the positive and negative best alternatives, which are used as references for the optimal [75].

2.8. Study on the Effect of Weight Reduction in Vehicles

Weight reduction in a vehicle plays a significant role in fuel consumption, and harmful gas emissions to the environment. When the weight is reduced the power, inertial forces, and energy required for engine, brake, and suspension systems are lowered. The reduction can be achieved by lightweight material substitution [1]. Based on this study 0.1kg weight reduction in an average vehicle's weight has an effect of 0.7L per 100km fuel consumption reduction. There are three strategies to reduce the weight of a vehicle, these are lightweight material substitution, vehicle design changes, and vehicle downsizing. Direct weight reduction or the substitution of lightweight material plays a great role in the industry [2]. Some components of vehicles like floors, roof panels, longitudinal front panels, firewalls, rear walls, and strut tower walls substitute currently lightweight materials rather than mostly made heavy weight and robust materials from steel and aluminum [3], [21].

Composite material has recently been used widely in automotive lightweight design to meet the worldwide top need for reducing carbon emissions to the environment and fuel consumption. Lightweighting of vehicles is one of the most realistic ways to meet these requirements due to the inherent relationship between mass and fuel consumption [76]. According to this journal, polymer composites can be a major part of the solution for the automotive industry's needs. Fiber-reinforced polymer composites present major lightweight opportunities for structural vehicle components. At a weight 50% lighter than conventional steel and 30%lighter than aluminum, more automakers use these materials as the body structure or other car components.

EDAG Silverado body light weighting final LCA report [77] has reported that the vehicle weight optimization method reduces fuel consumption and CO2 emissions to the environment. According to this report, the fuel savings for articulated trucks are estimated to be 0.03 liter per (100km x 100kg) on the flat 11 highway and up to 0.1 liter per (100km x 100kg) in urban traffic situations due to frequent accelerations, implying that the average fuel savings for trucks are about 0.06 liter per 100 km for a 100 kg weight reduction. Fuel consumption and CO2 emissions increase by about 6.5 percent for petrol engines and 7.1 percent for diesel engines for every 100 kg increase in mass. The more vehicle weight the higher the fuel consumption and CO2 emission.

More and more alternative lightweight materials are available, that can be used in the automotive industry, such as composite/polymer matrix material, high-strength steel (HSS), aluminum, magnesium, and so on. Usually, advanced materials have higher specific stiffness/strength than traditional materials. For some concept vehicles, the weight savings could reach 20% - 45% if advanced lightweight materials are used [78].

2.9. Study on the Analysis and Optimization of Composite's Structural Element

Structural elements are represented and idealized using mathematical models to simplify the analysis. A plate is a flat structural element characterized by small thickness compared with the surface and subjected to static or dynamic load only to in-plane loading, mainly concerned with perpendicular loads to the plate face or lateral loading [79], [80]. Thin plates combine light weight and form efficiency with high load-carrying capacity, economy, and technological effectiveness [80]. Problems of plates can be solved by classical plate theory.

Problems of rectangular plates clamped on four sides and carrying a uniformly distributed load maximum deflection were solved using the classical cosine series expansion method. A solution of governing equation interims of trigonometric and hyperbolic function result calculations for several ratios of a side of the plate was analyzed in a research study of an exact solution for the deflection of a clamped rectangular plate under uniform load [81].

The structural Analysis is performed for the Bus body superstructure [82], and the model is discretized into 241728 elements and 474933 nodes. Based on the Analytical results obtained by performing analysis on different locations (Cant rail, waist rail) of the Bus body superstructure. The bus body Superstructure is analyzed using ANSYS for materials like Carbon Fiber, Glass fiber, and Structural Steel, as per the result the maximum deformation that occurred for Structural steel and E-Glass is more compared to carbon fiber and E-Glass.

The basic principle of optimization is to find the best possible solution under given circumstances with the objective of maximization or minimization, Structural optimization is one application of optimization. Here the purpose is to find the optimal material distribution according to some given demands of a structure. Some common methods to minimize mass, displacement, or compliance

(strain energy). The main program used for performing finite element analyses and optimizations is the solver Optistruct 10.0 from Altair 17 Engineering [83].

Hypermesh is the preprocessor used to discretize (mesh) a CAD model, set boundary conditions, properties, and options, and set up the problem to be solved (optimization, static analysis, modal analysis, etc.). From Hypermesh a file that completely describes the problem is exported and then processed using Optistruct. The results from Optistruct can then be evaluated using the postprocessor Hyper View [83], [84]. The structural analysis of fiber-reinforced composite material utilizing the laminate theory and ANSYS finite element analysis methods for verifying the result and checking the failure of the ply laminate according to the Tsai-Wu failure theory for different stacking sequences [85].

2.10. Research Gap in Previous Research Works

Based on the reviewed research and literature, extensive studies have explored the combination of natural fibers (such as jute) with synthetic fibers (like PET) to create polymer composite materials, with a focus on characterizing their mechanical (e.g., strength, stiffness) and physical properties (e.g., durability, water absorption). However, these studies often conclude by suggesting that these hybrid composites could be used in lightweight vehicle components, without offering specific designs for particular applications. This represents a lack of detailed, practical designs for real-world applications. While these studies suggest potential uses in lightweight vehicle components (e.g., parts of cars or trucks), they generally do not provide concrete solutions.

Additionally, although significant research has been done on the chemical composition and recycling of PET fibers, there has been limited exploration of reusing PET by directly extracting it from plastic bottles. This method could contribute to reducing waste and enhancing the sustainability of composite materials. The gap in research is evident in the areas of simulation and experimental analysis of composite materials under various load conditions, particularly in automotive applications. Therefore, further work is needed to characterize, design, and optimize hybrid woven jute/PET composites for lightweight vehicles, to improve their strength-to-weight ratio for practical use.

CHAPTER THREE

3. METHODOLOGY

3.1. General Procedures

This chapter outlines the raw materials and fabrication of laminates, as well as the test setup and experimental findings related to the hybrid composites. The characterization of the laminates follows ASTM standards. The optimal laminate material is identified using the TOPSIS method, then designed and optimized with Optistruct, and validated through FEM analysis using ABAQUS. The figure below illustrates the research methodology flow.

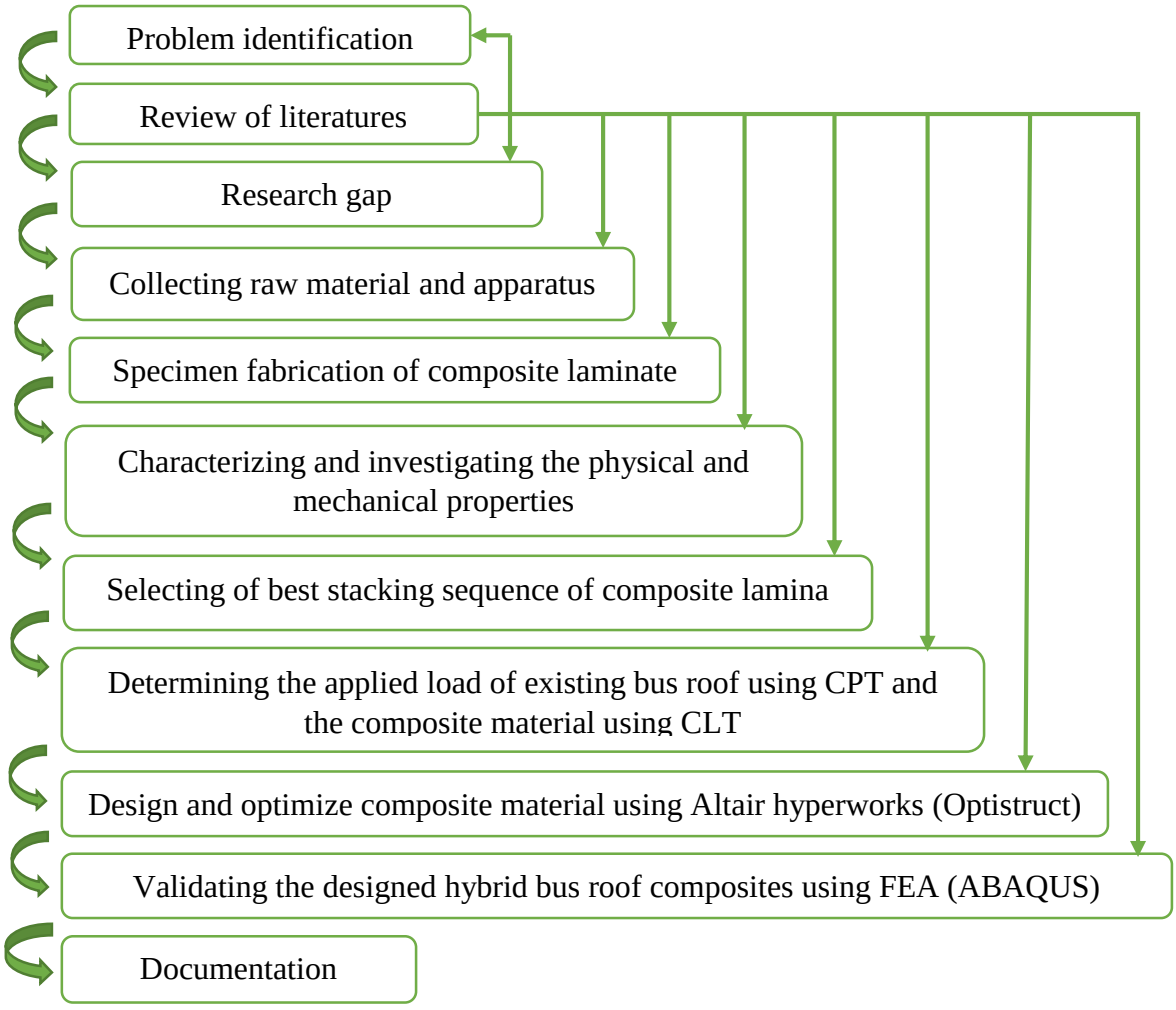

Figure 3-1: Research methodology flow diagram

3.2. Experimental procedures

The following sections provide a detailed overview of the apparatus, raw materials, and the method to manufacture composite laminates.

3.2.1. Apparatus

The apparatus used in this study was employed to prepare the raw materials for laminate production. The tools utilized for laminate preparation included scissors, gloves, a brush, a support table, a fine surface table, a plastic jar, a syringe, plaster, a hard flat plastic sheet, a ruler, a stick, an electronic balance, a roller, pressing weights, caliper, pincer, metal frame, screwdriver, screw nail, tape meter, disc cutter, and blade cutter.

Figure 3-2: Different Apparatus used for laminate preparation

3.2.2. Raw materials preparation

The main raw materials for this study include woven Jute fiber, PET fiber, Unsaturated General Polyester, Sodium hydroxide, and MEKP-Butanox M-50 hardener. Woven Jute fiber mats are purchased from the local market Mekelle. General polyester, Hardener (MEKP/Butanox M50), and releasing wax are purchased from Tiger Fiber Plc. in Mekelle. Also, Sodium hydroxide is used

from the Department of Chemical Engineering at Mekelle University. Whereas the Woven PET fiber is prepared from waste water plastic bottles manually.

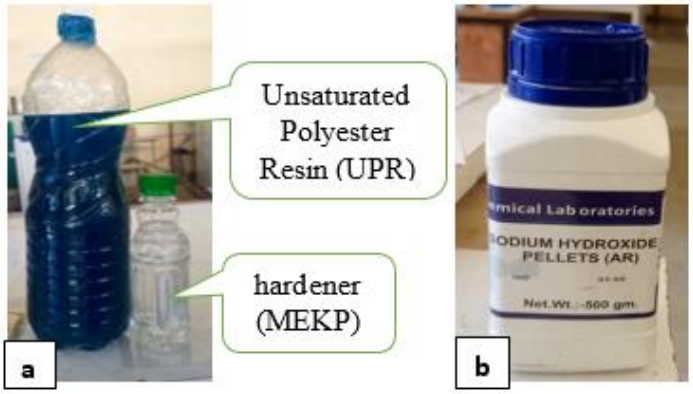

Figure 3-3: (a) general polyester resin and hardener, (b) sodium hydroxide pellets

A. Preparation of Woven PET fiber

To prepare the woven PET fiber, begin by collecting various waste plastic bottles, commonly known as "highland", and wash them thoroughly to remove dust and debris that could create voids or cavities in the laminate structure. After cleaning, cut the bottles into thin strips with an average width of 4 mm using a simple cutting mechanism in the workshop. Thin fiber composites generally outperform thick fiber composites in terms of strength, stiffness, and ductility [86], [87]. This is because thick fiber composites have fracture regions characterized by scattered bands of filaments, while thin fiber composites consist of more densely packed and overlapping filaments [87].

Figure 3-4: Collected different water plastic bottles

To produce PET fiber, insert the prepared plastic bottle into the central pillar, which enables rotation by pulling the fiber through the adjusted cutter positioned between the fixed plate and the cutter.

The gap between the fixed plate and the cutter is 4mm.

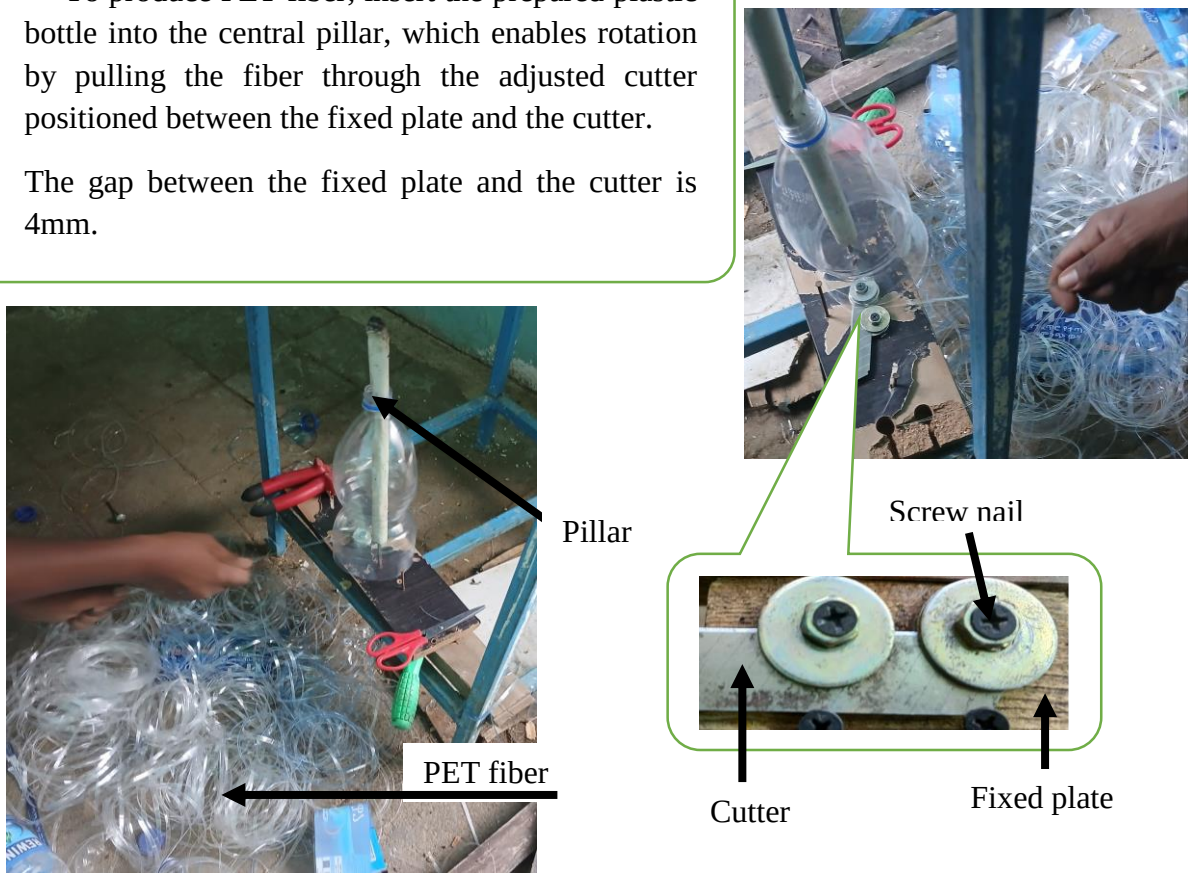

Figure 3-5: Plastic bottle cutting mechanism

Finally, manually weaving the thin PET strips into woven PET fiber. To make the woven fabric, start by creating a metal square frame measuring 350mm x 350mm to hold the thin PET strips. The woven fabric is formed by interlacing the yarns at right angles, typically 90 degrees, with the vertical threads referred to as "warp" and the horizontal threads called "weft". Woven fiber composites offer numerous advantages, such as fewer preforming process steps, good impact and delamination resistance, and strong thermo-mechanical properties. Woven hybrid fiber-reinforced composites exhibit superior properties because the loads applied to the composite surface are evenly distributed along the warp and weft directions of the fibers. This is particularly noticeable in impact resistance, where the interlocking of fibers enhances energy dissipation, leading to greater resistance [88].

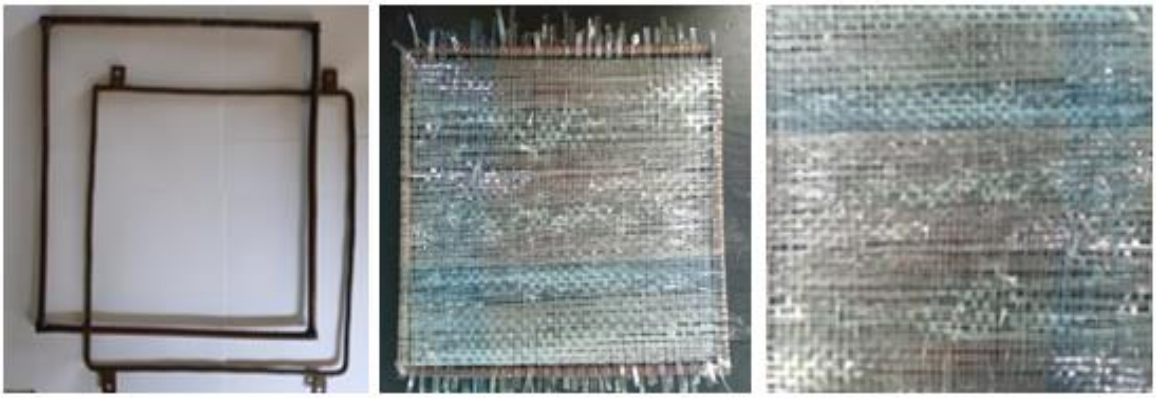

Figure 3-6: Metal frame and Hand made woven PET fiber

B. Alkali treatment of Jute fiber

The jute fiber was soaked in a 5% sodium hydroxide (NaOH) alkaline solution, prepared by dissolving 250g of NaOH pellets in water [28]. The fiber was immersed in the solution for 4 hours at room temperature. Subsequently, it was washed several times with clean water to eliminate any residual NaOH on the surface, and then dried in sunlight for up to 48 hours.

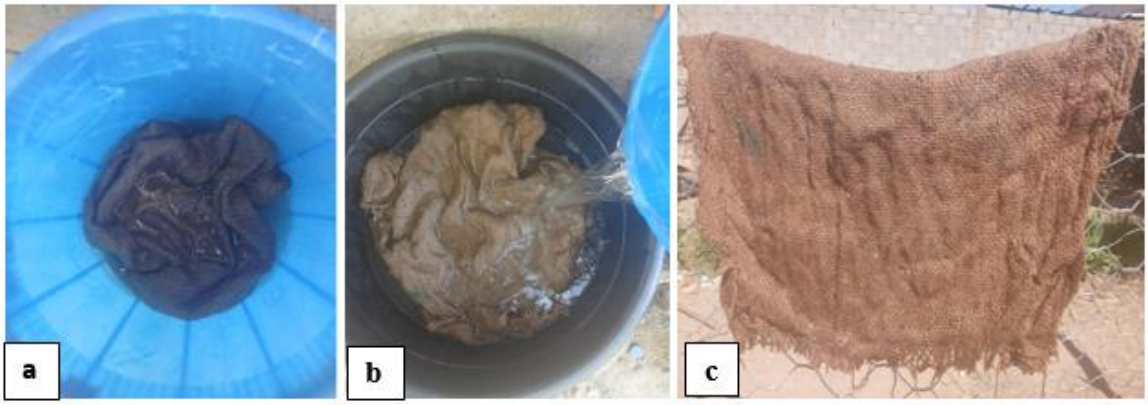

Figure 3-7: (a) jute immersed in the alkali solution and soaked (b) washed by pure water (c) fiber dried

C. Unsaturated Polyester Resin (Upr) - Hardener (Mekp/ Butanox M-50) Mixture

The resin utilized in this study was Unsaturated Polyester resin 1003, characterized by its low viscosity and formulated to produce minimal styrene emissions. Compared to standard resins, it demonstrates excellent mechanical and electrical properties, as well as strong chemical resistance. This resin serves as a matrix in composite materials, enhancing the strength and water absorption resistance of the composite laminate [88].

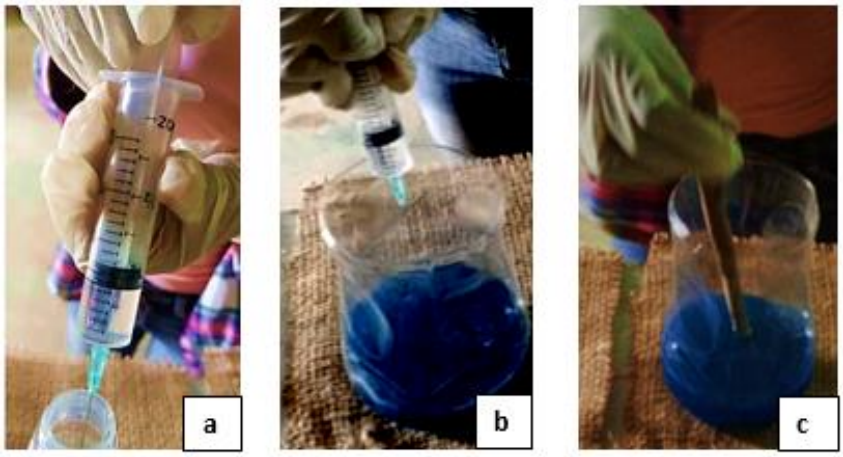

Figure 3-8: (a) measuring hardener (b) adding the hardener to polyester (c) and Mixing

Methyl Ethyl Ketone Peroxide (MEKP) serves as the curing agent for unsaturated polyester resins at room temperature, specifically the MEKP/Butanox M-50. In this study, 20 ml of MEKP-Butanox M-50 was used for every 1 kg of unsaturated polyester resin (UPR) [89], [90]. Then the mixture was gently stirred for about two minutes before being applied to the composite fiber in the mold.

D. Preparation of Jute and PET Fibers

The fibers (both treated and untreated jute fiber and PET fiber) were cut into 300 mm x 300 mm squares using scissors to prepare the samples. A tape meter and ruler were employed to measure the dimension of the specimens, while an electronic balance was used to determine their weight.

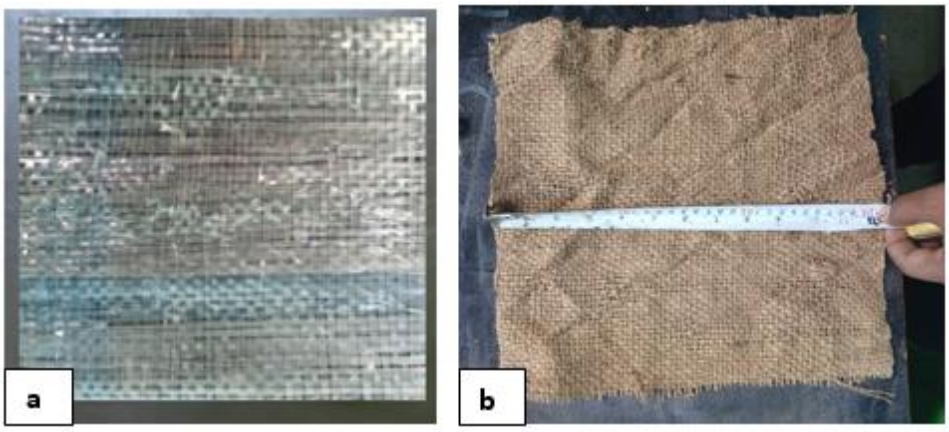

Figure 3-9: (a) woven PET fiber and (b) woven Jute fiber

3.2.3. Laminate Preparation

This research examined the physical and mechanical properties of the composite by creating various arrangements of jute and PET fibers for experimentation and analysis. To assess the mechanical properties of the samples, both alkaline-treated and untreated jute fibers were hybridized with woven PET fiber, following ASTM standards for design and fabrication. The composite was made using jute and woven PET fiber as reinforcement, with general polyester resin serving as the binder.

The fabrication of jute/PET fiber hybrid reinforced polyester composite was designed with the stacking sequences P-J-J-P, P-J-P-J, J-P-P-J containing alkaline-treated jute fiber lamina, P-J-J-P containing untreated jute fiber and also PET polyster (with out jute fiber). For each stacking sequence, the composites were reinforced with a jute/PET fiber [0^0, 0^0] orientation [17], [91].

Jute/PET fiber and matrix volume content determination

Determining the percentage composition of fiber to matrix ratio is the most important task in the fabrication and analysis of hybrid composite materials [91]. It was assumed that the fiber-reinforced hybrid composite performs perfect bonding between fibers and matrix, uniformity of fibers and free void throughout the matrix, the applied load is either parallel or normal to the fiber direction, stress-free state lamina and both fiber and matrix behave as linear elastic materials [16]. The fiber and matrix volume fraction of the hybrid composite was calculated by the rule of a mixture using the measured mass of the fibers and matrix on an electronic balance device [91]. The fiber density and matrix densities for PET fiber, jute fiber, and polyester resin were obtained from different literature reviewed as illustrated in Table below.

Table 3-1: Properties of raw materials

Material	Density (g/cm3)	Young's modulus (GPa)	Poisson's ratio	Shear modulus (GPa)	Reference
Jute fiber	1.4	26.5	0.25	0.5-2.5	[4], [29], [30], [31], [32]
PET fiber	1.35	2 - 3.50	0.39	1.375	[10], [56], [57],[58]
Polyester	1.25	3.2	0.36	0.8-3	[91], [92]

Thus, the volume fraction of jute fiber, PET fiber, and unsaturated polyester resin (UPR), was indicated in Table below.

Table 3-2: Experimental raw materials weight, weight fractions, and volume fractions

Stacking sequences	Mass (g) / Number of layers in the laminate(n)			Weight fraction (%)				Volume fraction (%)			
	m_j	m_{pet}	m_m	W_J	W_{pet}	W_f	W_m	V_J	V_{PET}	V_f	V_m
P-J-J-P (UJF)	109.4/2	81.6/2	286.5	22.91	17.08	40	60	21.24	16.43	37.7	62.3
J-P-P-J	104.6/2	82.4/2	280.5	22.37	17.62	40	60	20.74	16.94	37.7	62.3
P-J-J-P	103.6/2	83.4/2	280.5	22.16	17.84	40	60	20.54	17.15	37.7	62.3
P-J-P-J	103/2	82.6/2	278.4	22.19	17.8	40	60	20.58	17.11	37.7	62.3
PET Polyester	0	52.1	78.15	40	0	40	60	0	38.16	38.1	61.8

Where, m_j - jute mass, m_{pet} - PET mass, and m_m - matrix mass,

3.2.4. Sample fabrication procedures

The process of fabricating, forming, and shaping composite materials into final products is achieved through various methods. One of the most widely used and straightforward techniques is the hand lay-up method, which is commonly employed for producing both small and large reinforced thermoset-based fiber products [66]. In this study, the hand lay-up method is used to prepare composite laminates, as illustrated in the figure below. Composites with different compositions are created by reinforcing jute fiber, and PET fiber at 40%, with a polyester matrix making up 60%, based on weight percentage, and their mass is measured using an electronic balance.

Hard plastic sheets are placed on the top and bottom of the mold plate to ensure a smooth surface finish for the product. A release wax is applied to the plastic sheets used at the top and bottom of the mold plate to prevent the polyester from sticking to the mold surface and to achieve a good surface finish on the product. The fiber is then positioned on the mold surface, and then pouring the liquid polyester mixture onto the fiber. The polyester is evenly spread using a brush and roller to eliminate trapped air and excess polyester. This process is repeated for each layer according to the composite's stacking sequence. After covering the plastic sheet with a release wax, the top mold plate is positioned, and heavy pressure is applied. The mold is left to cure for 24 to 48 hours at room temperature before being opened and the finished composite part is removed. Finally, the

samples are cut for testing following ASTM standards [18][65]. The process was repeated for each sample of jute and PET fiber as per the orientation of the designed layers.

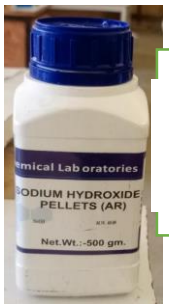

Alkaline for Treatment (NaOH)

Cutting the alkaline treated and untreated Jute & PET fiber to a size of 300 mm x 300 mm

Adding and mixing UPR with hardener (MEKP) then Stirring for a minute

Covering release wax to top and bottom mold hard plastic covered plates

Poured the resin mixture in the jute Layer and uniformly spread using brush

Adding the layers by their sequence & resin is spread uniformly with the help of roller

The top plate mold is covered and load pressure is applied.

Finished sample is takeout from the mold

Samples are cutted into specimens based on ASTM standards

Figure 3-10: Hybrid composite sample manufacturing process

3.3. Experiment to Determine Physical Property

3.3.1. Density of the Hybrid Composite

Density of composite is determined by the fraction of mass to volume of composite based on the ASTM D1895 standard [93]. The actual density (ρa) or experimental density of the composite was determined by the formula below;

$$\text{Density } \left({}^{g}/_{cm^3}\right) = {}^{m}/_{V} \quad \ldots\ldots\ldots\ldots\ldots\ldots\ldots\ldots (3.1)$$

Where m is the mass of the composite and V is the volume of the composite

Also, the theoretical density of the composite is determined by the equation of the Rule of Mixture [94]; Properties of fibers and matrix from table below;

$$\rho_{theoretical} = \frac{1}{\left[\left({}^{W_f}/_{\rho_f}\right) + \left({}^{W_m}/_{\rho_m}\right)\right]} \quad \ldots\ldots\ldots\ldots\ldots\ldots\ldots (3.2)$$

Where; W_f is the fiber weight fraction, ρ_f is fiber density, W_m is matrix weight fraction, and ρ_m is matrix density.

The rule of mixture allows the calculation of the approximate density of composite material based on the densities of individual components and their volume fractions in the composite. The densities of composite materials were normally measured using the Archimedes, and the density gradient method.

3.3.2. Water Absorption Testing

The water absorption test of jute and PET fiber-reinforced polyester composite materials was conducted by immersing the specimens in rainwater. pure water was selected to check the performance and applications of manufactured hybrid material in real-life conditions such as in rainy and humid environments Each sample was submerged for 24 hours at room temperature. After removal, the specimens were wiped dry and weighed daily over six days using a precise electronic scale to measure the amount of water absorbed. The weight changes were then used to calculate the water absorption percentage according to ASTM D570 standards, with the sample size being 76.2mm x 25.4mm x thickness (t mm) [95].

Figure 3-11: Samples are immersed in a water container

The water absorption percentages were subsequently determined as [94];

$$\text{Water absorption content, M, (\%)} = \frac{W_2 - W_1}{W_1} * 100 \quad \ldots\ldots\ldots\ldots\ldots\ldots (3.3)$$

Where W_2 and W_1 mass of the moist specimen after immersion and mass of dry specimen before immersion respectively.

3.4. Experiment to Determine Mechanical Property

The manufactured hybrid composite specimen was cut to the required dimension per ASTM testing guidelines using a disc cutter. Tensile testing, compression testing, and flexural testing were performed using Universal testing machines (Microcomputer Controlled Electro-Hydraulic Servo Universal Testing Machine, Model: SI-1000KN) and impact test was using charpy impact tester (Pendulum Impact Testing Machine, Model: SI-42, Impact Energy 150 J).

3.4.1. Tensile Testing

For tensile strength testing, a sample of the fabricated composite material was cut to dimensions of 250mm x 25mm x thickness (t mm) according to ASTM D3039 standards [96]. The test was conducted with a head displacement rate of 2mm/min and a gauge length of 150mm. Tensile testing evaluates the force required to break a composite or plastic sample, and how much the specimen elongates before rupture, providing data on its tensile strength, yield strength, and ductility [94]. The specimen was placed in a tensile testing machine, where tension was applied until the material broke.

Figure 3-12: Tensile testing using universal testing machine and Failure mode of specimens

3.4.2. Compression Testing

Composite compression testing methods apply a compressive load to the material while preventing it from buckling [94]. Compressive properties were determined by static compression test by ASTM D6641 [97]. A compression test was performed on a designed specimen with nominal geometrical dimensions of 50mm x 50mm x t mm, in which the maximum compressive strength and compression modules of the hybrid composite specimen were recorded.

3.4.3. Flexural Testing

The flexural test measures the force required to bend a beam under three-point loading conditions and measures the flexural stiffness and strength parameters of the hybrid polymer composite, as a result, the nominal specimen's geometrical dimensions were 150mm x 13mm x t mm as specified by ASTM D7264-07 standards [98]. Flexural strength is the ability of a material to bend before the breaking point. Bending strength was calculated from the data using the bending strength equation [94].

$$\sigma = {}^{3PL}/_{2bh}{}^{2} \quad \ldots\ldots\ldots\ldots\ldots\ldots (3.4)$$

Where: σ = stress at the outer surface at mid-span, P = applied force, L = support span, mm [in.], b = width, and h = thickness.

The specimen was horizontally mounted on two supports in the flexural testing and the load was then slowly increased to the center of the specimen with a speed of 5mm/min.

3.4.4. Impact Testing

The Charpy impact test measures the energy absorbed during fracture under an impact load, helping to assess the material's fracture toughness. The material's ability to resist a sudden applied load was tested using a Charpy impact testing machine (Pendulum Impact Testing Machine, Model: SI-42, Impact Energy 150 J) [94]. Five un-notched specimens were prepared according to ISO 179/92 (2010) or ASTM D 256 standards [99], with dimensions of 80mm x 10mm x thickness (t mm) for each composite laminate. The impact strength was calculated by dividing the absorbed energy by the cross-sectional area of each specimen.

Figure 3-13: Charpy impact testing machine and Failure mode of specimens

3.5. Application of the TOPSIS method

All the fabricated samples were characterized and investigated their mechanical and physical properties were based on the test requirement of ASTM standards. Selecting the best laminate stacking sequence from the different alternatives based on the criteria using the TOPSIS technique helps in decision-making. The selection of evaluation criteria depends on the specific objective and requirements of the composite material application. The criteria taken to compute the composite laminates are (tensile strength, compressive strength, flexural strength, impact strength, water absorption, and density).

TOPSIS method involves some steps; these are as follows [73], [74].

Step 1: Establishing a decision matrix for ranking consisting of alternatives and criteria.

Step 2: Construct the normalized decision matrix

Step 3: Determine the weighted normalized decision matrix

The bus roof loading plate application is always related to the impact-loading type. In this study, based on the relative importance of criteria to the specific application area of top bus roof load plate its material properties of tensile, compressive, flexural strength, and cost, weighted as 0.15 to each, impact strength as 0.2, water absorption, and density as 0.1.

Step 4: Calculate the positive (best) ideal solutions (V+) and negative (worst) ideal solutions (V-) for each criterion from the alternatives.

Step 5: Calculate the Euclidean distance between the target alternative and the best/worst alternative Si+/Si- separation measure value using the Euclidean distance method.

Step 6: Determine the relative closeness to the ideal solution for each alternative.

Step 7: Finally Rank the preference order. A large value of the closeness coefficient indicates a good performance of the alternative. The best alternative is the one with the greatest relative closeness to the ideal solution.

3.6. Determining the Applied Load on the Existing Bus roof plate

To determine the applied load, the existing input data were acquired from the ISUZU company websites [100], and the importing company found in Addis Ababa's local market is given in the Table below.

Table 3-3: The input data of modified ISUZU NPR71 4570cc buses

Model name	ISUZU NPR71
Engine capacity CC	4570 cc
Gross Vehicle weight	6 tonne
Maximum loading capacity	3 tonne
Roof size	6.7m X 2 m
Thickness	2mm – 3 mm
The density of the Mild steel	7850kg/m3
Young's modulus	200Gpa
Poisson's ratio	0.303
Upper loading box size (a x b)	1.20m X 2.80m
Maximum loading capacity on upper loading box	550 Kg

The length and width dimension of the plate surface is much greater than its thickness, so it is a thin plate and it is solved using classical plate theory. Assumption of classical thin plate theory of fully supported plate [101], [102];

- The material is homogeneous and isotropic.
- The thickness of the plate is much smaller than the in-plane dimensions.
- The deformations of the plate surface are small compared to the plate thickness.
- Vertical deflection does not vary through the thickness.
- Normal to the undeformed plate surface remains normal to the deformed plate surface.
- Transverse loads applied at the shear center prevent torsion or twist in the structure
- The mid-plane is a natural plane
- Stress, normal to the plate surface is negligible
- The self-weight of the plate is ignored.

Since the top roof is fully supported by the bus body frame (structure), it is modeled as fixed in all edge plates with uniformly distributed load applied on the loading box only. According to Timoshenko the deflection and moments of uniformly loaded and all-edge built-in rectangular plates are symmetrical to the coordinate axes [101].

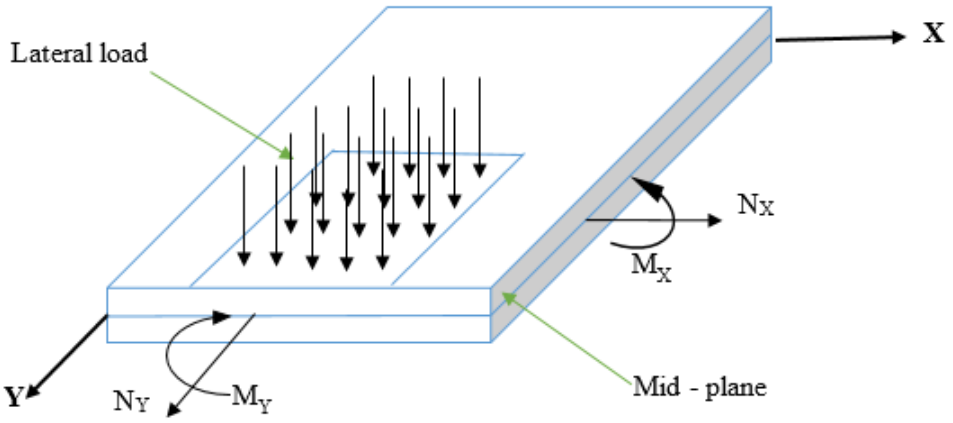

Figure 3-14: In-plane normal forces and bending moments diagram

Moment–curvature equations for a plate can be expressed in the following equation [81];

$$M_X = -\int_{-h/2}^{h/2} \sigma_X Z dZ = -\int_{-h/2}^{h/2} \left[-\frac{2E}{1-v^2}\left(\frac{\partial^2 w_0}{\partial x^2} + v\frac{\partial^2 w_0}{\partial y^2}\right)\right] Z dZ = \frac{Eh^2}{12(1-v^2)}\left[\frac{\partial^2 w_0}{\partial x^2} + v\frac{\partial^2 w_0}{\partial y^2}\right]$$

$$\boldsymbol{M_X = D\left[\frac{\partial^2 w_0}{\partial x^2} + v\frac{\partial^2 w_0}{\partial y^2}\right]} \quad \ldots\ldots\ldots\ldots\ldots\ldots\ldots\ldots (3.5)$$

$$M_Y = -\int_{-h/2}^{h/2} \sigma_Y Z dZ = -\int_{-h/2}^{h/2} \left[-\frac{2E}{1-v^2}\left(\frac{\partial^2 w_0}{\partial y^2} + v\frac{\partial^2 w_0}{\partial x^2}\right)\right] Z dZ = \frac{Eh^2}{12(1-v^2)}\left[\frac{\partial^2 w_0}{\partial y^2} + v\frac{\partial^2 w_0}{\partial x^2}\right]$$

$$\boldsymbol{M_Y = D\left[\frac{\partial^2 w_0}{\partial y^2} + v\frac{\partial^2 w_0}{\partial x^2}\right]} \quad \ldots\ldots\ldots\ldots\ldots\ldots\ldots\ldots (3.6)$$

Where factor ***D*** is called plate stiffness or bending rigidity.

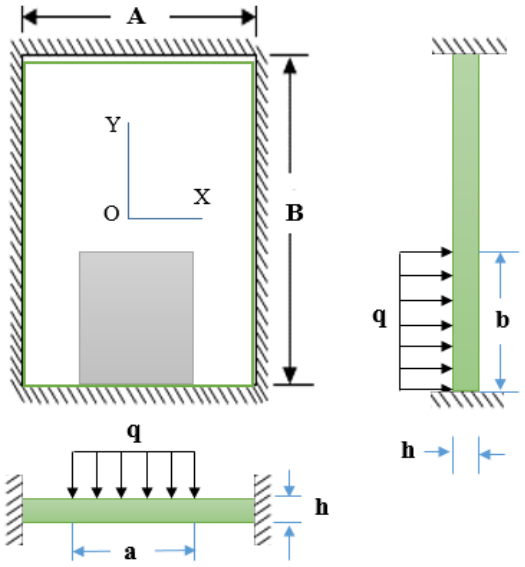

Figure 3-15: FBD of a rectangular thin plate fixed in all edges and load distribution

The above figure shows the distributed load subjected to the existing loading box of the top roof of the bus. Using the simplified equation below, the maximum load applied on the loading box of the bus is 5395.5 N and the distributed weight on the loading box of the bus will be 1605.80 N/m^2.

$$F = Maximum\ applied\ load\ \times g = 550\ Kg\ \times 9.81\ {}^{m}/_{s^2} = 5395.5\ N \quad \ldots\ldots\ldots (3.7)$$

$$q = {}^{F}/_{Area\ of\ the\ plate} = {}^{5395.5\ N}/_{(1.2\ m\ \times 2.8m)} = {}^{1605.80\ N}/_{m^2} \quad \ldots\ldots\ldots (3.8)$$

Normal forces per unit length of sections of a plate perpendicular to x and y direction, N_x and N_y respectively.

$$N_X = {}^{F}/_{a} = 4496.25\ {}^{N}/_{m} \ldots\ldots\ldots (3.9)$$

$$N_Y = {}^{F}/_{b} = 1926.96\ {}^{N}/_{m} \ldots\ldots\ldots (3.10)$$

Bending moments per unit length of sections of a plate perpendicular to the x and y axes, Mx and My respectively. The coefficients of length-to-width ratio α and β of 1.1 are given [103];

$$M_{center} = \alpha qab, \quad \text{And} \quad M_{edge} = \beta qab \ldots\ldots\ldots\ldots (3.11)$$

$$M_X = \beta_a qab = -0.0392qab = -211.5\ \text{Nm/m}$$

$$M_X = \alpha_a qab = 0.0183qab = 98.74\ \text{Nm/m}$$

$$M_Y = \beta_b qab = -0.0098qab = -52.87\ \text{Nm/m}$$

$$M_Y = \alpha_b qab = 0.00461qab = 24.87\ \text{Nm/m}$$

Maximum stress has occurred at the mid-edge of b,

$$\sigma_{max} = \frac{qa^2}{2t^2(0.623(\frac{a}{b})^6 + 1)} = 127.97Mpa \ldots\ldots\ldots\ldots (3.12)$$

Maximum deflection also occurs at the center,

$$\Delta_{max} = \frac{0.0284qa^4}{Et^2(1.056\left(\frac{a}{b}\right)^5 + 1)} = 0.517465\ x\ 10^{-6}\ m \ldots\ldots\ldots\ldots (3.13)$$

3.7. Design of Hybrid Laminate Composite Bus Roof

The design and analysis of laminated structures involve examining strength, stresses, and strain distribution using Classical Laminate Theory (CLT) and Finite Element Analysis (FEA). Mechanical structures experience external forces that result in internal forces within the body [104]. In this study, hybrid jute and PET fiber laminates with 0° ply orientations were created, consisting of four fiber layers bonded with a polyester matrix. The fiber stacking sequence of

Woven P-J-J-P was selected using the TOPSIS method. The laminate was designed symmetrically, with equal ply dimensions above and below the mid-plane, all having 0° orientations. The schematic below illustrates the four-layer composite in a symmetric configuration.

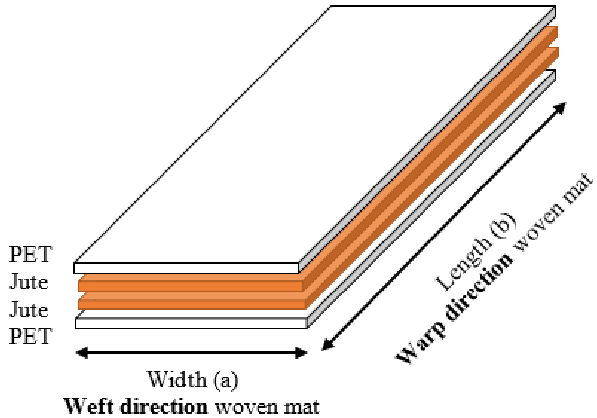

Figure 3-16: Stacking sequence and orientation of the fabricated composite sample

Assumptions taken for the laminate composite [15], [104];

- Each lamina (layer) of the laminate is a quasi-homogeneous material with known effective properties and orthotropic.
- The laminate consists of perfectly bonded layers.
- Individual layer properties can be isotropic, orthotropic, or transversely isotropic.
- The displacements are continuous throughout the laminate.
- Normal distances from the middle surface constant, that is, the transverse normal strain ε_z is zero and each layer is in a state of plane stress.
- Each displacement is small compared with the thickness of the laminate$|u|, |v|, |w| \ll h$.
- The stress-strain and strain displacement are linear.
- The plate is considered to be under plane stress; That is, $\sigma_3 = \tau_{13} = \tau_{23} = 0$

Stress-strain Relationship for Orthographic Lamina

For a thin layer of the composite lamina, it can be assumed that the lamina is under plane stress conditions in the direction of lamina thickness [101]. The stress-strain relationship in principal material generalized by Hooke's law for orthotropic material is given by:

$$\{\sigma\} = [Q]\{\varepsilon\} \qquad \ldots (3.14)$$

Where; the stress-strain relationship can be expressed in the matrix as follow:

$$\begin{Bmatrix}\sigma_1\\ \sigma_2\\ \sigma_3\\ \tau_{12}\\ \tau_{13}\\ \tau_{23}\end{Bmatrix} = \begin{bmatrix}Q_{11} & Q_{12} & 0 & 0 & 0 & 0\\ Q_{12} & Q_{22} & 0 & 0 & 0 & 0\\ 0 & 0 & Q_{33} & 0 & 0 & 0\\ 0 & 0 & 0 & Q_{44} & 0 & 0\\ 0 & 0 & 0 & 0 & Q_{55} & 0\\ 0 & 0 & 0 & 0 & 0 & Q_{66}\end{bmatrix} \begin{Bmatrix}\varepsilon_1\\ \varepsilon_2\\ \varepsilon_3\\ \gamma_{12}\\ \gamma_{13}\\ \gamma_{23}\end{Bmatrix} \dots\dots\dots\dots (3.15)$$

Where $[Q_{ij}]$ is a reduced-stiffness matrix and the subscripts 1, 2, and 6 refer to the properties along the fiber, transverse to the fiber, and shear in the plane respectively.

The plane is under plane stress condition, all the stress components in the out-of-plane direction are zero. Therefore, the minimized stress-strain relationship in the matrix form is given by;

$$\begin{bmatrix}\sigma_1\\ \sigma_2\\ \tau_{12}\end{bmatrix} = \begin{bmatrix}Q_{11} & Q_{12} & 0\\ Q_{12} & Q_{22} & 0\\ 0 & 0 & Q_{66}\end{bmatrix} \begin{bmatrix}\varepsilon_1\\ \varepsilon_2\\ \gamma_{12}\end{bmatrix} \qquad \dots\dots\dots\dots\dots\dots\dots\dots (3.16)$$

Where E_1 and E_2 are the young's moduli of lamina along the longitudinal and transverse to the fiber direction, respectively. v_{12} is Poisson's ratio and G_{12} is the shear modulus of lamina under a loading along the fiber direction.

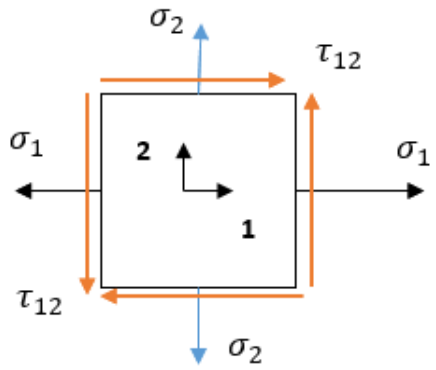

Figure 3-17: Longitudinal (σ_1), transverse (σ_2) and shear stress (τ_{12})

The matrix Q_{ij} depends on the material properties and it is given in terms of engineering constants as follows;

$$Q_{11} = \frac{E_1}{1 - v_{12}^2 \frac{E_2}{E_1}}, \quad Q_{12} = \frac{v_{12}E_2}{1 - v_{12}^2 \frac{E_2}{E_1}}, Q_{22} = \frac{E_2}{1 - v_{12}^2 \frac{E_2}{E_1}}, and\ Q_{66} = G_{12} \dots\dots (3.17)$$

Analytical calculation using the rule of mixture equation, the material properties of E_1, E_2, v_{12}, and G_{12} each ply is calculated using the equations below to find the value of the reduced stiffness matrix $[Q_{ij}]$ for each ply, E_1, E_2, v_{12}, and G_{12} in table A-2 in the Appendix A.

Young's modulus;

$$E_1 = E_f E_m + E_m V_m \; and \; E_2 = \frac{E_m E_f}{E_f V_m + E_m V_F} \qquad \ldots\ldots\ldots\ldots\ldots\ldots\ldots (3.18)$$

Poisson's Ratio;

$$v_{12} = v_f V_f + v_m V_m \; and \; v_{21} = \frac{E_2 v_{12}}{E_1} \qquad \ldots\ldots\ldots\ldots\ldots\ldots\ldots\ldots (3.19)$$

Shear modulus;

$$G = \frac{E}{2(1+v)} \qquad and \qquad G_{12} = \frac{G_m G_f}{G_f V_m + G_m V_f} \qquad \ldots\ldots\ldots\ldots\ldots\ldots\ldots (3.20)$$

The stiffness matrix of each ply is calculated using,

$$[Q] = \begin{bmatrix} Q_{11} & Q_{12} & Q_{16} \\ Q_{12} & Q_{22} & Q_{26} \\ Q_{16} & Q_{26} & Q_{66} \end{bmatrix} \qquad \ldots\ldots\ldots\ldots\ldots\ldots\ldots\ldots\ldots\ldots (3.21)$$

Force and Moment Resultants Related to Mid-plane Strains and Curvatures

The mid-plane strains and mid-surface curvatures can be found using the ABD matrix which is a 6x6 matrix that the applied loads and the associated strains in the laminate. It essentially defines the elastic properties of the entire laminate. [A], [B], [D] are called extensional, coupling, and bending stiffness matrices respectively, their formulas are described in Appendix C. The stress, resultant force, and moment relationships for laminate are given as follows.

$$\begin{bmatrix} N \\ M \end{bmatrix} = \begin{bmatrix} [A] & [B] \\ [B] & [D] \end{bmatrix} \begin{bmatrix} \varepsilon^0 \\ k \end{bmatrix} \qquad \ldots\ldots\ldots\ldots\ldots (3.22)$$

According to lamination theory, stiffness matrices are generally derived relative to the mid-plane of a laminate. A laminate is considered symmetric when each layer on one side of the reference plane (the middle surface) has a corresponding layer on the opposite side at an equal distance, with identical thickness, orientation, and material properties.

In the case of symmetric laminates, the coupling stiffness matrix [B] equals zero, indicating no coupling between bending and stretching. Consequently, in-plane loads do not induce bending or twisting curvatures that could lead to out-of-plane deformation, and bending or twisting moments do not produce strain in the middle surface. When subjected solely to forces, a symmetric laminate will exhibit zero curvature at the mid-plane; when subjected only to moments, it will experience zero mid-plane strains. The laminate's structural response is characterized by the strains and

curvatures at its mid-plane, and global stresses (such as those from angle plies) are calculated based on these mid-plane strains and curvatures.

$$\begin{bmatrix}\sigma_x\\ \sigma_y\\ \tau_{xy}\end{bmatrix} = \begin{bmatrix}\bar{Q}_{11} & \bar{Q}_{12} & \bar{Q}_{16}\\ \bar{Q}_{12} & \bar{Q}_{22} & \bar{Q}_{26}\\ \bar{Q}_{16} & \bar{Q}_{26} & \bar{Q}_{66}\end{bmatrix}\begin{bmatrix}\varepsilon_x\\ \varepsilon_y\\ \gamma_{xy}\end{bmatrix} \quad \ldots\ldots\ldots\ldots\ldots\ldots (3.23)$$

And

$$\begin{bmatrix}\varepsilon_x\\ \varepsilon_y\\ \gamma_{xy}\end{bmatrix} = \begin{bmatrix}\varepsilon_{x0}\\ \varepsilon_{y0}\\ \gamma_{xy0}\end{bmatrix} + Z\begin{bmatrix}k_x\\ k_y\\ k_{xy}\end{bmatrix} \quad \ldots\ldots\ldots\ldots\ldots\ldots (3.24)$$

Where $\varepsilon_{x0}, \varepsilon_{y0,}$ and γ_{xy0} the mid-plane strains $k_x, k_{y,}$ and k_{xy} are the mid-plane curvatures, Z is the coordinate measured from the mid-plane to the lamina and $\varepsilon_x, \varepsilon_y$ and ε_{xy} are the strains in the k_{xy} ply.

The above equation indicates the linear relationship of the strain to the curvatures of the laminate. Where ($\varepsilon_{x0}, \varepsilon_{y0,}$ and γ_{xy0}) are the mid-plane strains and ($k_x, k_{y,}$ and k_{xy}) are the mid-plane curvatures, Z is the coordinate measured from the mid-plane to the lamina. The global and local coordinate systems are related by the angle at which the lamina is placed (θ). Using a transformation matrix, it is possible to convert the global stress in a laminate into the local of a lamina.

$$[T] = \begin{bmatrix}\mathrm{m}^2 & \mathrm{n}^2 & 2\mathrm{mn}\\ \mathrm{n}^2 & \mathrm{m}^2 & -2\mathrm{mn}\\ -\mathrm{mn} & \mathrm{mn} & \mathrm{m}-\mathrm{n}^2\end{bmatrix} \quad \ldots\ldots\ldots\ldots\ldots (3.25)$$

Where; m = cos θ and n = sin θ

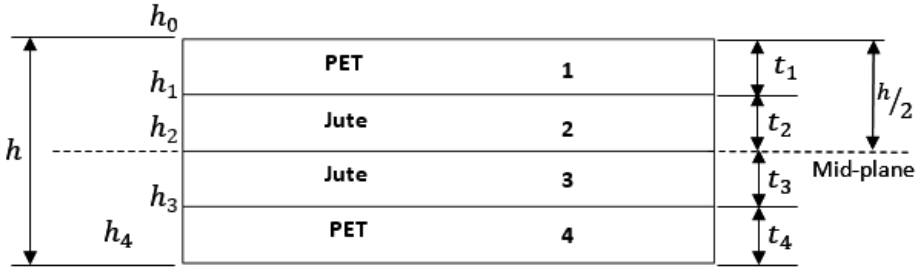

Figure 3-18: Coordinate locations of plies in a laminate

The laminate extensional stiffness matrix can be calculated by using the stiffness matrixes and the position and thickness of the lamina. [A], [B], and [D] matrix is given by;

$$[\mathrm{A}] = \sum_{\mathrm{k}=1}^{4}\left[\bar{\mathrm{Q}}_{\mathrm{ij}}\right]_{\mathrm{k}} (\mathrm{Z}_{\mathrm{k}} - \mathrm{Z}_{\mathrm{k}-1}), \mathrm{i}, \mathrm{j} = 1,2,6 \quad \ldots\ldots\ldots\ldots\ldots\ldots (3.26)$$

$$[B] = \frac{1}{2}\sum_{k=1}^{4}\left[\bar{Q}_{ij}\right]_k \left(Z_k{}^2 - Z_{k-1}{}^2\right), i,j = 1,2,6 \quad \ldots\ldots\ldots\ldots\ldots (3.27)$$

$$[D] = \frac{1}{3}\sum_{k=1}^{4}\left[\bar{Q}_{ij}\right]_k \left(Z_k{}^3 - Z_{k-1}{}^3\right), i,j = 1,2,6 \quad \ldots\ldots\ldots\ldots\ldots (3.28)$$

The mid-plane strain and plate curvature are calculated to determine the global and local stress and strains. The values of global, and local strains and stresses of each ply are detailed and calculated as shown in Appendix C to predict the performance of the hybrid composite.

Failure theories are developed to compare the stresses in the material with the failure criteria. The Tsai-Wu failure theory was used as a constraint throughout the analysis and optimization of the bus roof plate. Tsai-Wu failure theory is based on the total strain energy failure theory to lamina in the plane stress, and the lamina fails if (3.29) is violated.

$$g(u) = F_1\sigma_1 + F_2\sigma_2 + F_6\sigma_{12} + F_{11}{\sigma_1}^2 + F_{22}{\sigma_2}^2 + F_{66}{\sigma_{12}}^2 + F_{12}\sigma_1\sigma_2 \leq 1 \quad \ldots\ldots (3.29)$$

Where, $F_1, F_2, F_6, F_{11}, F_{22}, F_{66}$ *and* F_{12} were the components of the failure theory parameters found using the five strength parameters in Appendix C, table C-1.

Strength Ratio

If SR>1 then the lamina is safe and the applied stress can be increased by a factor of SR. If the $SR < 1$the lamina is unsafe and the applied stress needs to be reduced by a factor of SR.

$$SR = \frac{Ultimate\ stress}{Applied\ stress} > 1 \qquad \ldots\ldots\ldots\ldots\ldots (3.30)$$

3.8. HyperWorks-Optistruct Modeling, Analysis & Optimization of Plate Composite

Altair HyperWorks 2019 software is utilized for the design analysis and optimization of hybrid composites. The composite part's finite element model is created in HyperMesh, where the properties of each lamina are inputted, and the user profile preferences are set to OptiStruct. For the model, PET/polyester lamina and jute/polyester lamina material types are used, with their respective properties provided in Tables A-2 and C-1 in Appendix A and C. The software enables the modeling of the hybrid composite structure and the creation of its mesh. Once the model is constructed using the input data in HyperMesh, it is ready for structural analysis.

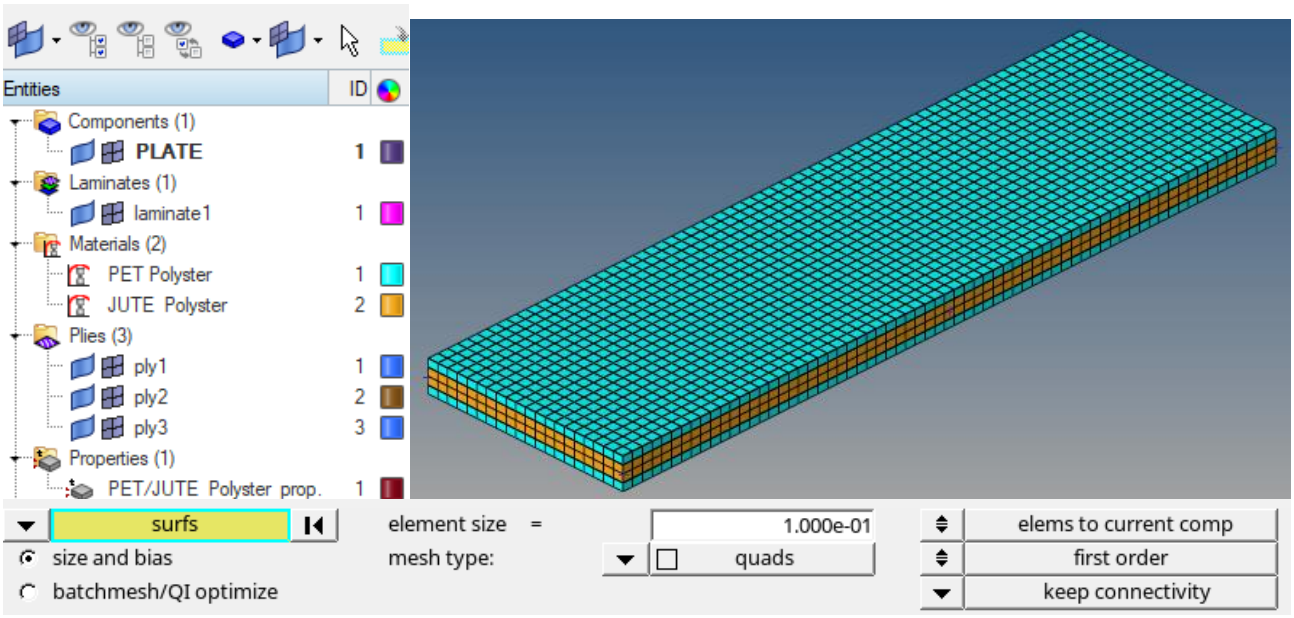

Figure 3-19: Model browser and hyper mesh hybrid composite plate model

Defining boundary conditions and loads

Since the plate is fully supported, It is fixed on all edges, and the maximum load applied is distributed to the number of elements created on the plate as shown in Figure 3.17.

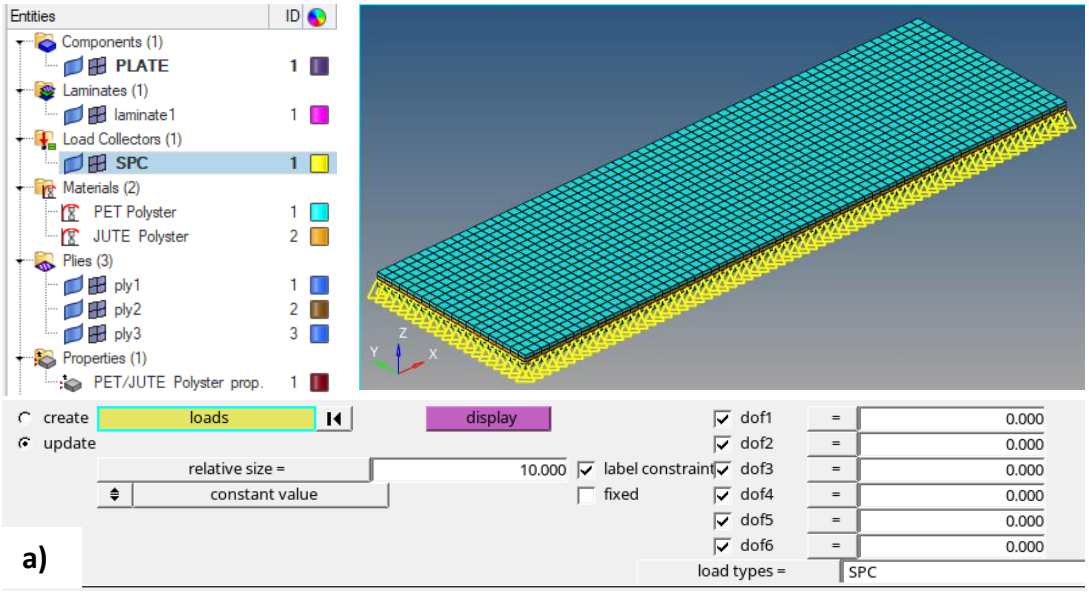

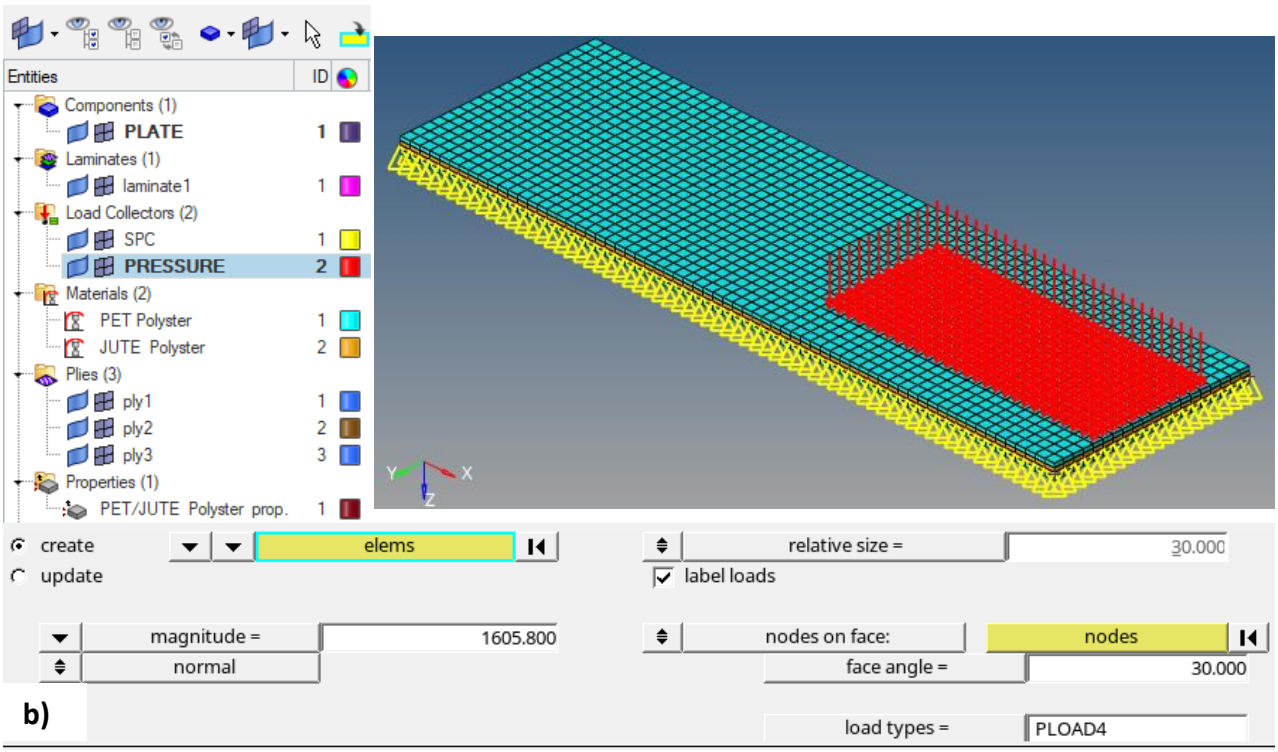

Figure 3-20: (a) Applying BCs, and (b) Load applied to the laminate

Altair OptiStruct offers extensive optimization capabilities to select the best possible options while considering the imposed constraints and desired objectives, ultimately improving composite models [83], [84]. The free-size optimization (FZO) in OptiStruct optimizes the thickness of each ply on an element-by-element basis, subject to an upper bound. The free-size optimization problem consists of the following components:

Design Variables are system parameters that can vary to optimize system performance which change to get the best of several possible design configurations. In this study, the design variable is the thickness of each ply and lamina angle orientation.

$$T_i^L < t_i < T_i^U \dots\dots\dots i = 1,2,3,\dots n \quad \dots\dots\dots\dots\dots\dots\dots\dots (3.31)$$

Continuous variation of thickness offers move design freedom, because of FZO t_i allows to vary freely between the lower, T_i^L and upper bound thickness, T_i^U. The discrete solution is achieved by penalizing intermediate thickness (taking average thickness).

$$\text{Angle orientation} = [\min(\sigma_c)] = [\max(\text{FS})] \dots\dots\dots (3.32)$$

FZO optimizes the angle indirectly by comparing the maximum element composite stress resulting from the optimized thickness that creates the minimum stress distribution developed in the structure to have a greater factor of safety.

Responses are any value or function measurable in the problem parameters that are dependent on the Design Variable and evaluated during the solution. For this study, the responses are mass, and composite failure index.

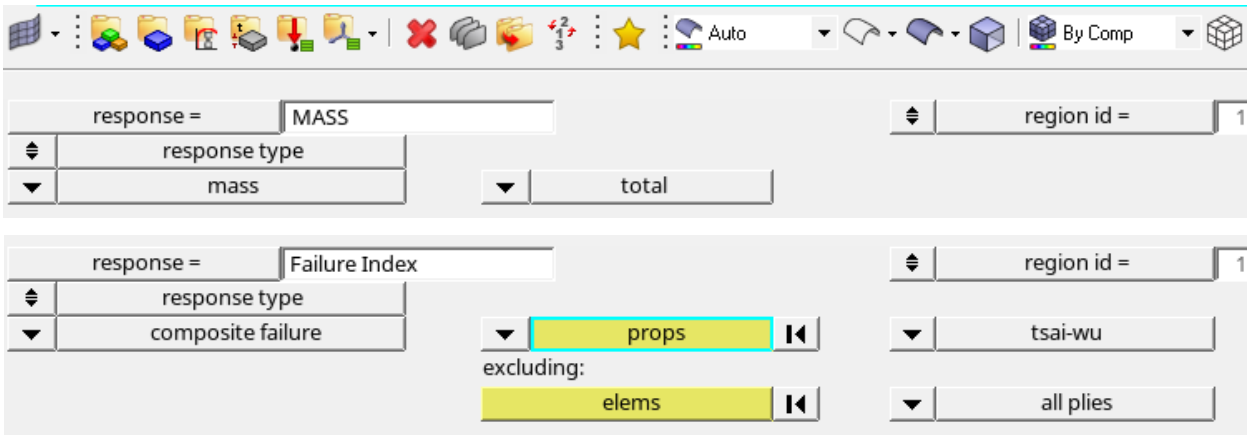

Figure 3-21: Design Response for Optimization

Constraints represent a lower or upper limit on any response that depends on the design variable. In this study, the constraint applied to the analysis for determining the optimized bus roof plate was the Tsai-Wu failure theory equation, which relies on the material properties of the laminate composite.

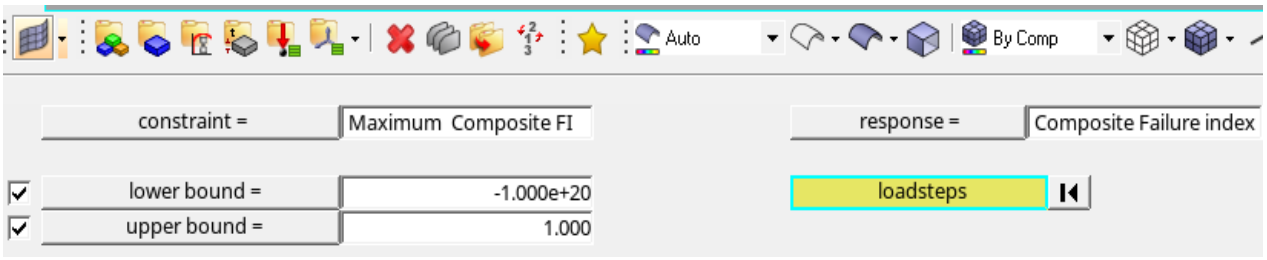

Figure 3-22: Design Constraint for Optimization

Objectives In design optimization, the objective function is minimized (or maximized) while adhering to performance constraints by varying the set of design variables, such as part dimensions, material properties, and others. The primary goal of this thesis is to achieve a bus roof plate with a minimum weight-to-strength ratio.

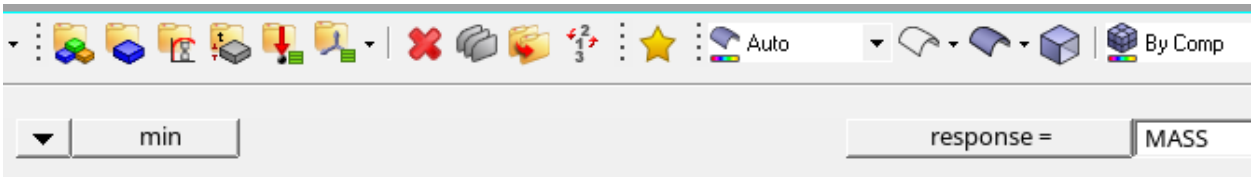

Figure 3-23: Design Objective for Optimization

The input file for all Optistruct optimizations is provided in Appendix D and was used to optimize the thickness and minimize the overall weight of the loading floor plate.

3.9. Validation using ABAQUS software

To validate the result the optimized loading floor plate is re-analyzed using ABAQUS 2022 for validation.

Model

The figure below depicts the structural configuration of the Jute-PET composite plate, along with the layering sequence of the ply laminate (P-J-P), which consists of plies oriented at 0°, 90°, 0°.

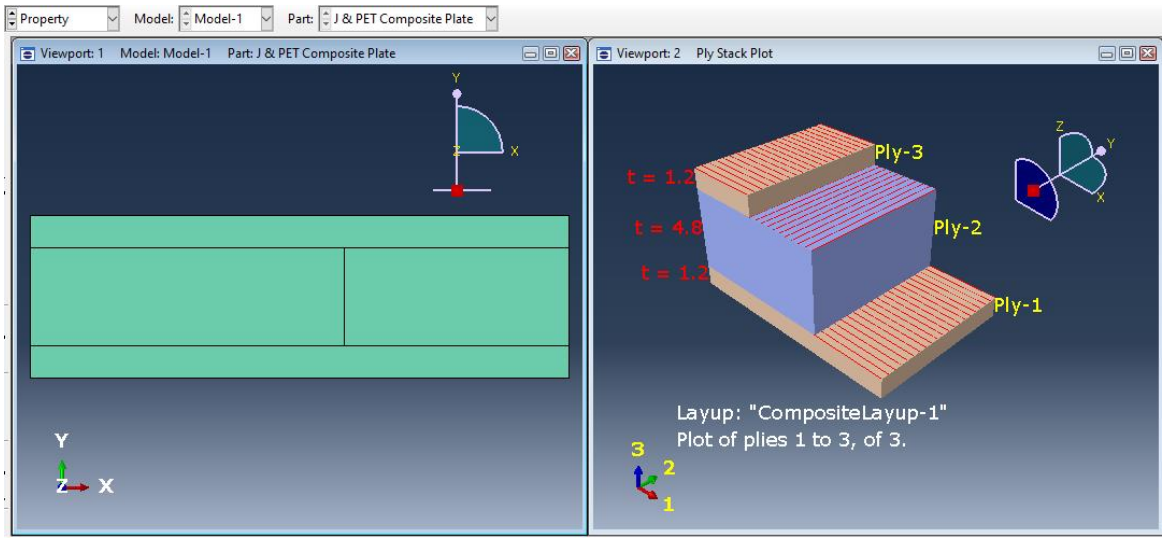

Figure 3-24: Optimized 3D model and ply stacking sequence of the bus roof plate

Meshing

Meshing entails breaking down the solids or surfaces into individual elements. This was done using the S4R linear mesh element type, which is a 4-node, doubly curved shell capable of handling both thin and thick structures. It incorporates reduced integration, hourglass control, finite membrane strains, and a mesh size of 0.05.

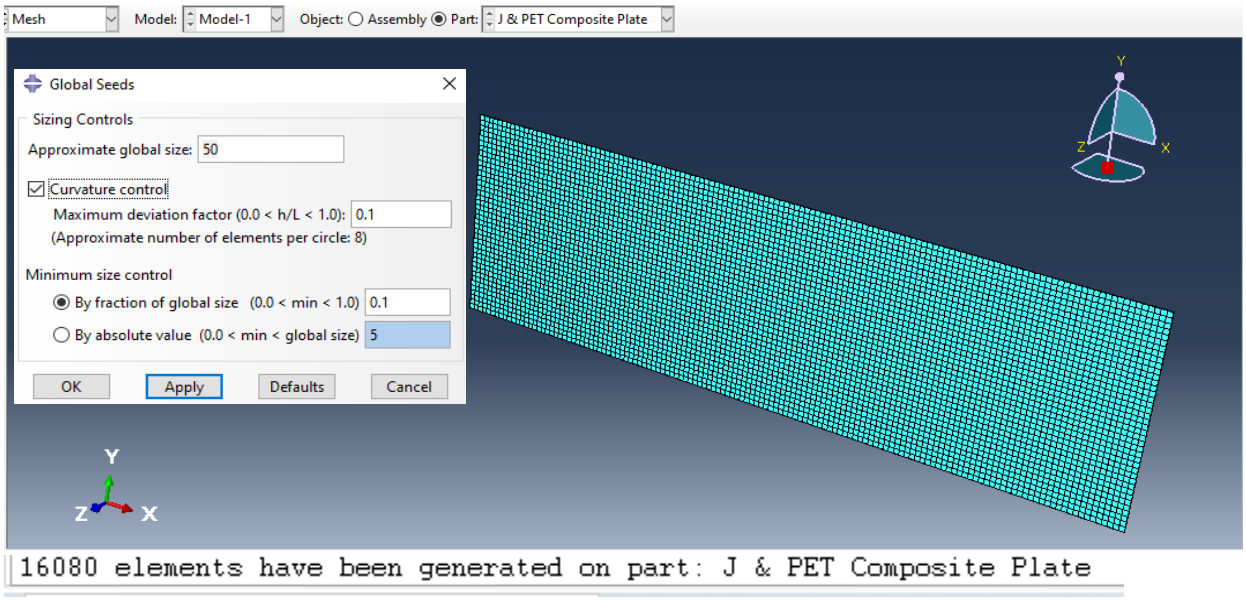

Figure 3-25: Meshing using 3D element

Defining applied load

In this step, the applied load and the constraints are defined. The distributed load is applied on the structural plate and designed for static load. and the constraints are defined as fixed in all edges and distributed load $1605.80\,N/m^2$.

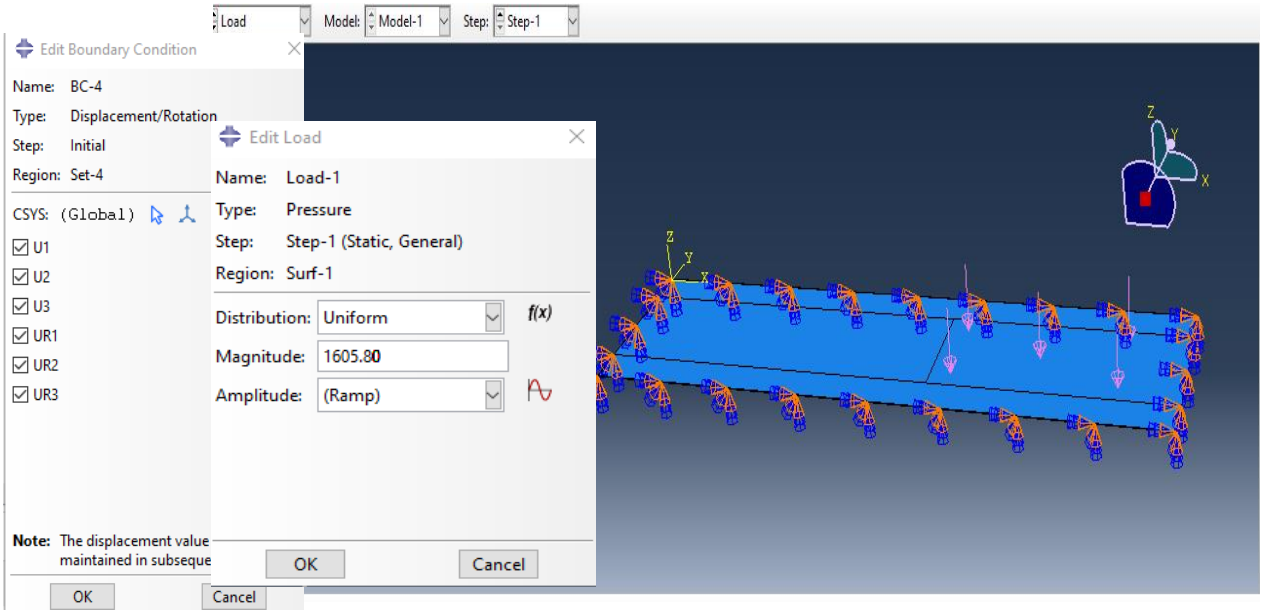

Figure 3-26: Load defining

CHAPTER- FOUR

4. RESULT AND DISCUSSION

4.1. Introduction

This chapter presents the results from various sample tests on composite materials with fiber-to-matrix weight fractions ranging from 40% to 60%. It also analyzes the laminated structure of bus roof plates using Classic Laminate Theory and Tsai-Wu failure theory. The bus roof plate is designed based on experimental data and the properties of the composite materials. An optimization study was conducted using Altair Hyperworks-Optistruct software to reduce the weight of the bus roof plate structure. The optimized design is then validated through Abaqus software. The results are summarized and discussed in the following sections.

4.2. Physical Property

4.2.1. Density

The density of each specimen is measured according to the procedures outlined in the materials and methods chapter of this thesis. The composite laminate has a density of 1297.8 kg/m^3. A comparison of the experimental and theoretical densities is provided in the summary table (A-1) in Appendix A. The results show that the theoretical densities are higher than the experimental values, as the effects of voids and porosity are not considered in the theoretical calculations.

4.2.2. Water absorption

The amount of water absorbed by a particular specimen depends upon the total reinforcement in the composite and the jute fibers' weight percentage [17]. The results revealed that the Jute/PET fiber reinforced composite with a P-J-J-P sequence absorbed 1.13% of water after 144 hours of immersion in rainwater, while the hybrid composite with the same sequence but using untreated jute fiber absorbed 2.13% over the same period. This suggests that the untreated fibers exhibited a notable increase in water absorption, while alkali treatment of the fibers significantly reduced water absorption by sealing the fiber-matrix interfaces and minimizing voids. In the J-P-P-J sequence, the water absorption rate is 3.13%, whereas the P-J-J-P sequence had a lower absorption rate of 1.13%. This suggests that the outer PET fiber significantly reduces water absorption, as laminating it on the outer surface of the composite lowers jute fiber's absorption.

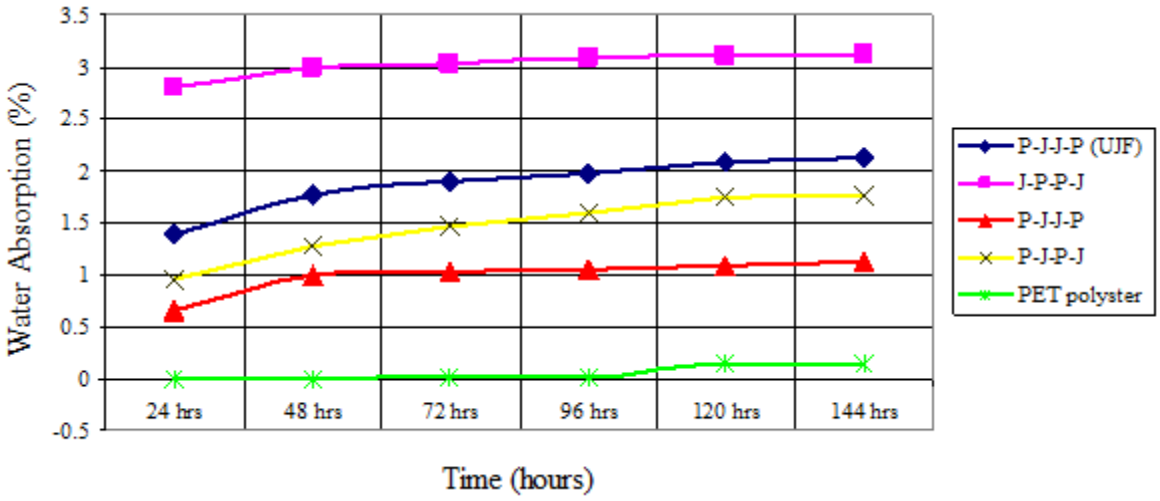

Figure 4-1: Water Absorption Results Diagram

In contrast, when the outer layer is made of natural fiber, water absorption increases due to its hydrophilic nature. On the other hand, the water absorption rate of PET polyester is nearly zero, as polyester is generally hydrophobic and does not absorb water easily, instead transferring moisture to adjacent fibers.

4.3. Mechanical Properties

4.3.1. Tensile Strength Test Result

Figure 4.2 illustrates the tensile strength of various jute/PET hybrid reinforced composite materials. The composite with an alkaline-treated jute fiber inner layer (P-J-J-P) exhibits the highest tensile strength, 107.4 MPa, among all the tested samples. In contrast, the PET polyester-only composites have the lowest tensile strength, 48.4 MPa.

The alkaline treatment of the jute fiber significantly improves the tensile strength by 28.2% in the P-J-J-P composite. Therefore, treating natural jute fiber gives a better tensile property for the composite. Generally, tensile strength increases when alkali-treated fiber is used which increases the interfacial bonding between fiber-matrix adhesion. The jute fibers in the outer layers of the specimens are less capable of handling high loads, resulting in the PET fibers bearing most of the stress. However, alkaline-treated jute fibers perform better under stress than untreated jute in composites with identical stacking sequences.

Composites with outer PET fiber layers (e.g., P-J-P-J) demonstrate superior mechanical properties compared to other configurations. For instance, the ultimate tensile strength of the P-J-P-J

composite is 91.6 MPa, higher than the 77.3 MPa of the J-P-P-J hybrid. Overall, hybridizing jute with PET polyester matrix increases in tensile strength, with an improvement of 121.9% (from 48.4 MPa to 107.4 MPa).

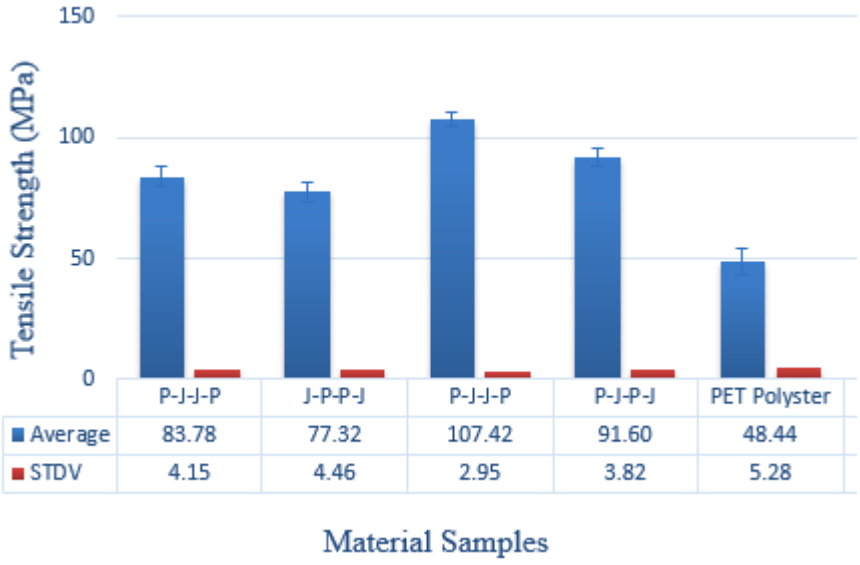

Figure 4-2: Average tensile strength test results

4.3.2. Compression Strength Test Result

Figure 4.3 illustrates that the J-P-P-J hybrid reinforced fiber specimen has a relatively low average compressive strength of 38.3 MPa, while the P-J-J-P hybrid specimen with alkaline-treated jute fiber achieves the highest compressive strength of 56.2 MPa. The compressive strength of the P-J-J-P composite with alkaline-treated jute fiber is 14.4% greater than that of the untreated jute fiber in the same configuration and 7.66% higher than the treated jute fiber in the P-J-P-J sequence. This shows that treated jute fiber improves the compressive properties of the composite. Compressive strength increases with alkali treatments of the fiber. Conversely, untreated jute fibers in the P-J-J-P hybrid provide a 28.2% higher compressive strength than the J-P-P-J hybrid. This suggests that the outer PET fiber layers significantly contribute to improved compressive strength, likely due to their lower water absorption properties.

Overall, combining alkaline-treated jute fibers with a PET polyester matrix leads to a significant enhancement in compressive strength, showing a 112.87% increase (from 26.4 MPa to 56.2 MPa).

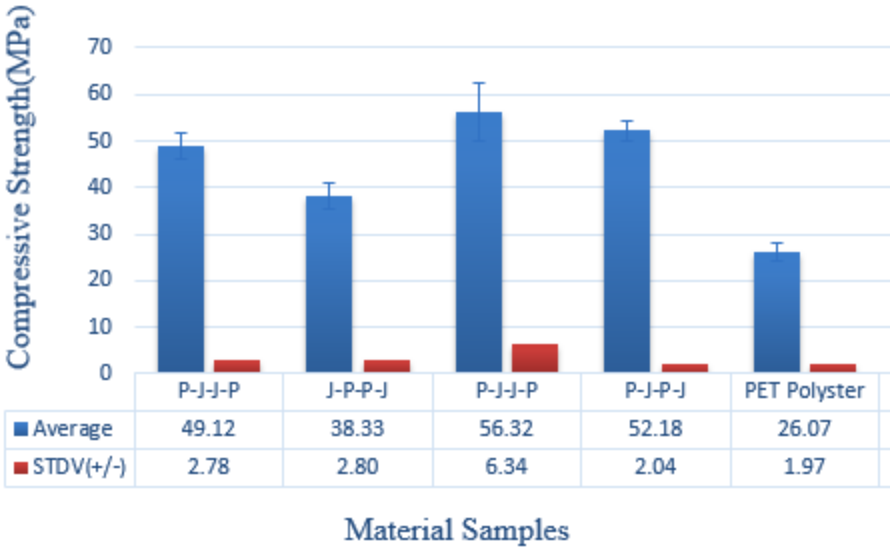

Figure 4-3: Compressive Strength test results

4.3.3. Flexural Strength Test Result

Figure 4.4 presents the results of a three-point bending flexural test, comparing the flexural strength of various composite materials. All composites, whether reinforced with treated or untreated jute fibers in combination with PET fibers and matrix, demonstrated strong flexural performance. Among the tested hybrids, the P-J-J-P stacking sequence exhibited the highest flexural strength, attributed to the two layers of alkaline-treated jute fiber in the outer layers, complemented by PET fibers. Alkaline treatment of the jute fiber resulted in a 4.15% increase in flexural strength, rising from 183.6 MPa (P-J-J-P UJF) to 191.2 MPa (P-J-J-P).

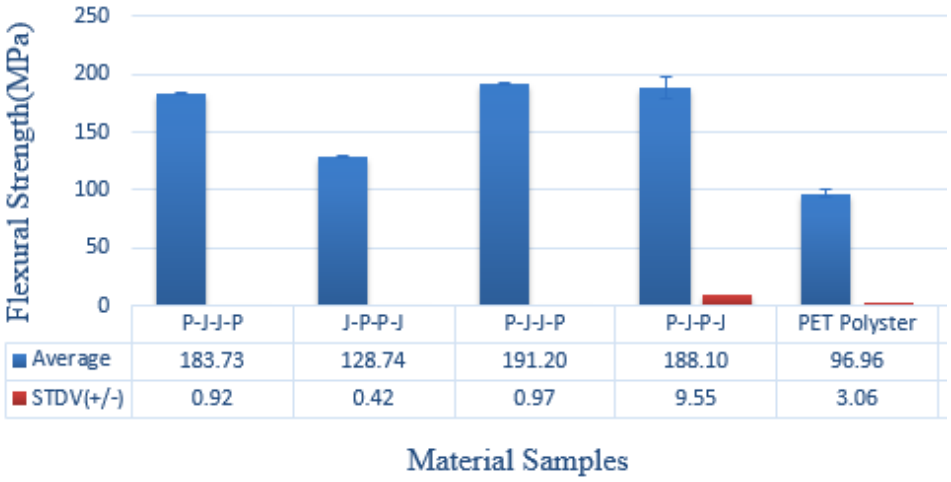

Figure 4-4: Flexural strength test result

In general, the hybridization of alkaline-treated jute fibers with a PET polyester matrix leads to a substantial improvement in flexural strength, with an increase of 95.5% (from 97.8 to 191.2 MPa).

4.3.4. Impact Strength Test Result

Figure 4.5 presents experimental results indicating that alkaline-treated jute fiber hybridized with PET fiber exhibits slightly higher impact strength compared to composites made with untreated jute fiber. Specifically, the untreated jute fiber in the P-J-J-P composites results in an impact strength of 79.8 MPa, while the alkaline-treated jute fiber in the same stacking sequence reaches a maximum impact strength of 81.3 MPa. This improvement is due to the enhanced mechanical properties of the jute fibers after alkaline treatment.

Additionally, the impact strength of composites with alkaline-treated jute fiber in the outer layers is lower than that of composites with PET fiber in the outer layers. For example, the P-J-P-J composite, with PET fiber as the outer layer, shows an impact strength of 74.6 MPa, which is lower than the 81.3 MPa of the P-J-J-P composite with treated jute fibers. However, it is slightly higher than the 71.3 MPa observed in the J-P-P-J composites. This difference is attributed to the fact that PET fibers in the outer layers absorb more impact energy than jute fibers.

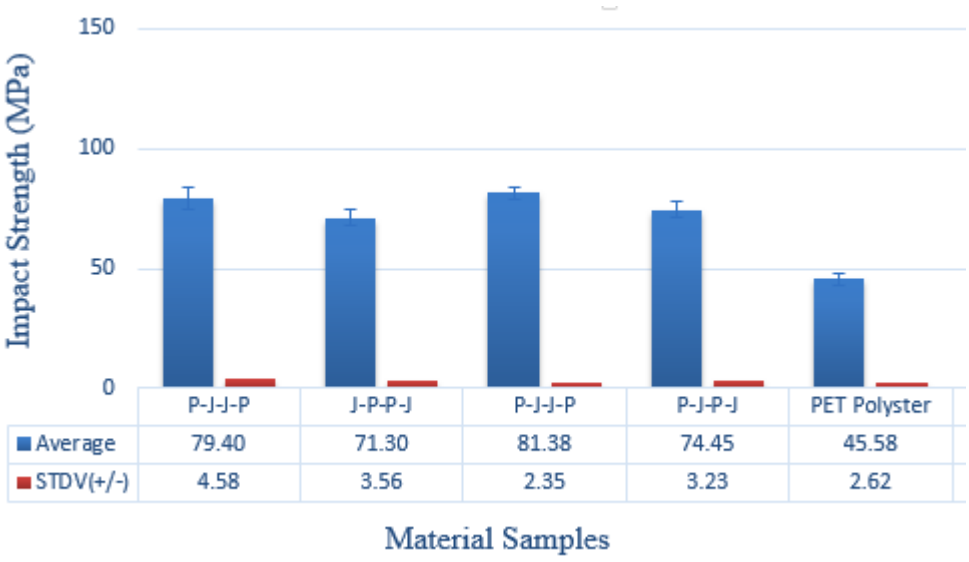

Figure 4-5: Impact strength test result

In general, the hybridization of alkaline-treated jute fibers with a PET polyester matrix leads to a substantial enhancement in impact strength, with an increase of 78.68 % (from 45.5 to 81.3 MPa).

4.4. TOPSIS analysis method

The steps of the decision-making technique and the resulting outcome are provided in Appendix B. It was found that the optimal laminate composite stacking sequence, chosen from five different fabricated sample alternatives (P-J-J-P (UJF), J-P-P-J, P-J-J-P, P-J-P-J, and PET polyester), based on mechanical and physical properties (tensile, compressive, flexural, impact strength, water absorption, and density), is **P-J-J-P**. This sequence, a woven jute/PET polyester hybrid reinforced composite, demonstrated superior properties and higher strength than all the other samples.

4.5. Hyperwork-Optistruct analysis and optimization

A model was developed to assess stress and strain in four-layered, angle-ply symmetric laminated plates. The numerical analysis used classical lamination theory to calculate resultant forces and bending moments, determining stresses and strains per ply. HyperWorks (OptiStruct) analysis revealed that the 0°, 90°, and 0° P-J-P ply orientation yielded the lowest maximum stress and failure index. This configuration was selected as optimal, as detailed in Table 4.1. From analyzing the strength ratio, the PET-J-PET composite achieved its highest value (SR = 2.658) at an angle orientation of 0°, 90°, and 0°. This suggests that the maximum elemental stress within the plate is reduced more effectively at this specific angle compared to other orientations. The composite exhibited maximum stress and strain values of 21.14 MPa and 1.871e-3, respectively.

Table 4-1: Optistruct Analysis Result

Angle orientation of P-J-P	**Maximum element stresss(MPa)**	**Maximum composite strain**	**Composite failure index (FI)**	**Factor of safety**
0^0, 0^0, 0^0	21.78	1.869E-3	0.06041	2.580
0^0, 30^0, 0^0	21.92	1.854E-3	0.05968	2.563
0^0, 45^0, 0^0	21.95	1.847E-3	0.05978	2.560
0^0, 90^0, 0^0	**21.14**	**1.871E-3**	**0.0581**	**2.658**
30^0, 0^0, 30^0	23.79	1.890E-3	0.1318	2.362
30^0, 30^0, 30^0	23.98	1.893E-3	0.1324	2.343
30^0, 45^0, 30^0	24.07	1.901E-3	0.1339	2.334
30^0, 90^0, 30^0	23.69	1.921E-3	0.1391	2.372
45^0, 0, 45^0	24.37	2.059E-3	0.2138	2.306
45^0, 45^0, 45^0	24.75	2.079E-3	0.2179	2.270
45^0, 90^0, 45^0	24.29	2.104E-3	0.2276	2.313
60^0, 0^0, 60^0	23.79	2.218E-3	0.2303	2.362

60^0, 45^0, 60^0	24.25	2.236E-3	0.2354	2.317
60^0, 90^0, 60^0	23.71	2.282E-3	0.2481	2.370
90^0,0^0,90^0	25.31	2.231E-3	0.07804	2.220
90^0,45^0,90^0	26.06	2.231E-3	0.07994	2.156
90^0,90^0,90^0	26.64	2.134E-3	0.08385	2.109

The HyperWorks (OptiStruct) analysis for the 0°, 90°, and 0° P-J-P ply orientation is illustrated in the figure below, providing detailed insights into the stress and strain distribution.

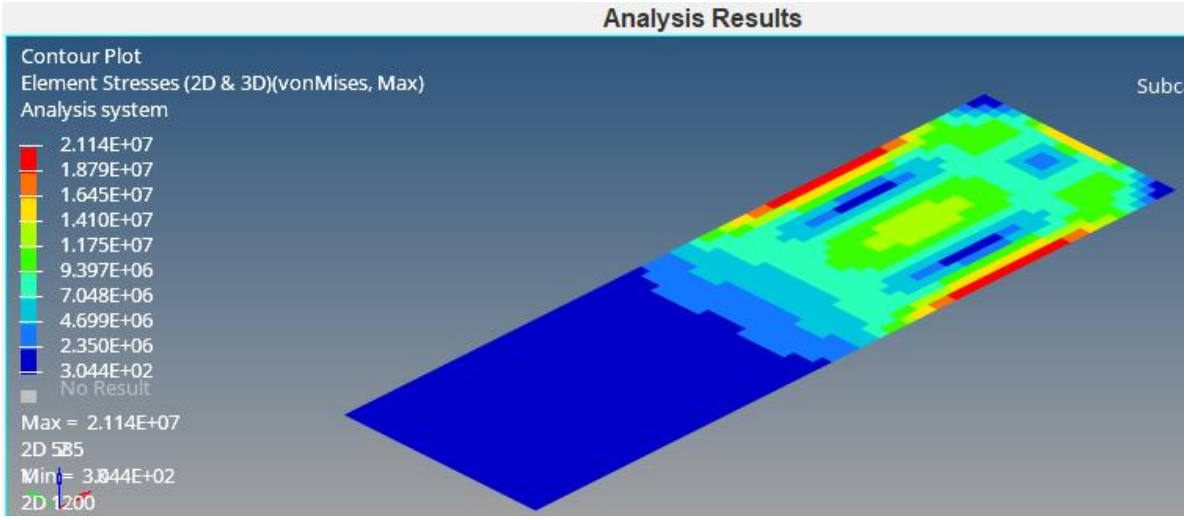

Figure 4-6: Composite element stresses analysis result of composite laminate

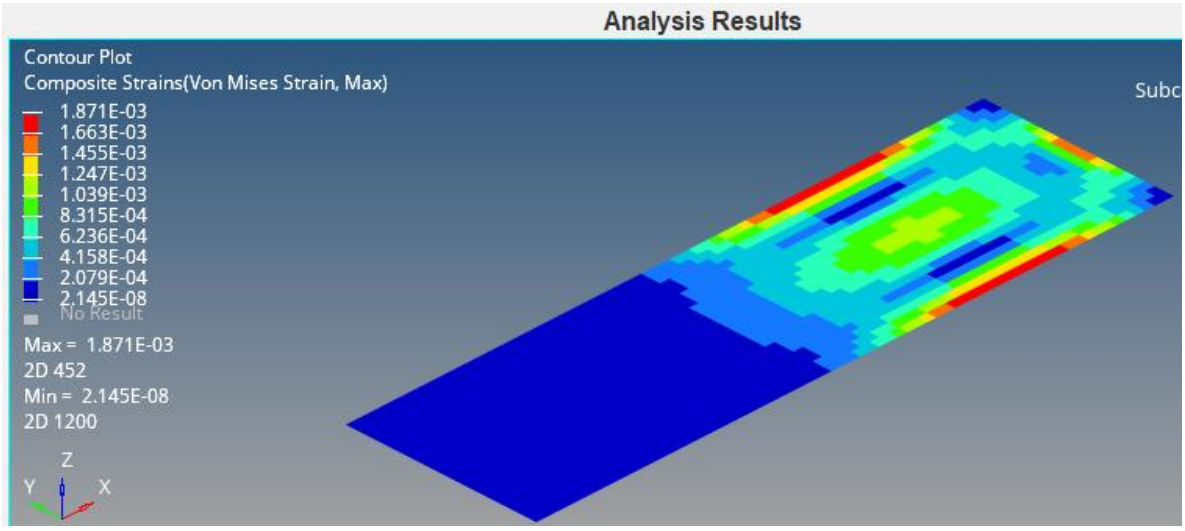

Figure 4-7: Composite strains analysis result of composite laminate

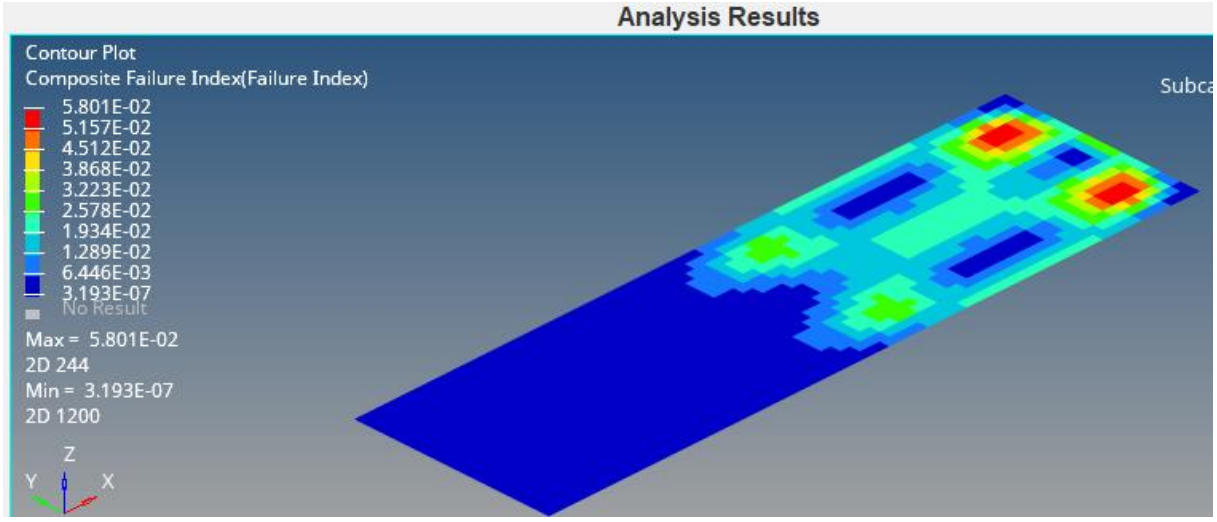

Figure 4-8: Composite FI result

Using thickness and angle orientation as design variables in Optistruct optimization for the composite plate, the process begins by adjusting the thickness to reduce weight, as illustrated in Figure 4.9., Iteration 4 achieves the first satisfactory convergence ratio, reducing the mass to 137.63 kg. Subsequently, the stress distribution in the optimized structure is assessed by iteratively modifying the ply angle orientations, specifically testing the PET-J-PET arrangement at 0°, 90°, and 0°.

```
ITERATION    4

Objective Function (Minimize MASS ) =  1.37635E+02   % change =       -1.04
Maximum Constraint Violation %      =  0.00000E+00
Design Volume Fraction              =  7.50000E-02   Mass     =  1.37635E+02

 Subcase    Compliance     Epsilon
       1  4.703389E+02  9.006211E-13

Note : Epsilon = Residual Strain Energy Ratio.
```

Figure 4-9: Optistruct Optimization Result

The optimized thickness results show that the PET polyester laminate on the outer surfaces specifically plies one and three, is 1.2 mm, while the jute polyester laminate in the middle layer, ply two, has a thickness of 4.8 mm. This configuration results in a total mass of 137.63 kg. The total mass of the existing (mild steel) bus roof plate is 210.38 Kg. Considering the optimized hybrid composite laminate for the bus roof plate without changing the structure achieved 34.58% mass saving compared to steel.

$$Volume_{mild\ steel} = 6.7m \times 2m \times 0.002m = 0.0268m^3$$

$$Mass_{mild\ steel} = 0.0268m^3 \times 7850\ {}^{Kg}/_{m^3} = 210.38\ Kg$$

Table 4-2: Mass comparisons

Type	Mass (Kg)	% reduced
Mild steel	210.38	0%
Optimised composite	137.63	34.58%

This reduction in mass not only enhances fuel efficiency and reduces operational costs but also contributes to the vehicle's overall sustainability and minimises its environmental impact. The lighter weight of the optimised composite improves vehicle efficiency, delivering both economic and environmental advantages. Theoretical fuel savings can be estimated using the formula provided below [21].

$$\text{Average fuel saving} = \frac{0.38\ \text{L} * \text{reduced mass}}{100\text{kg} * 100\text{km}} \quad \ldots\ldots\ldots\ldots (4.36)$$

$$\text{reduced mass} = 210.38\text{Kg} - 137.63\text{Kg} = 72.75\text{Kg}$$

$$\text{Average fuel saving} = \frac{0.38\ \text{L} * 72.75\text{Kg}}{100\text{kg} * 100\text{km}} = \frac{0.2765\ litre}{100Km}$$

An average fuel saved of 0.2765 litre/100 Km was achieved by the optimised composite bus roof for the ISUZU NPR71 4570cc buses.

4.6. Validation of results using Abaqus software

The Analysis and optimisation were done using Hyperworks-Optistruct software. Here, to confirm the results the optimised bus roof is analysed again using ABAQUS 2022 for validation purposes.

1. Von Mises Stresses on each ply

The Von Mises stress is a measure of equivalent stress that cumulates the impact of all individual stress components.

PET fiber-reinforced polyester plies (ply-1 and ply-3)

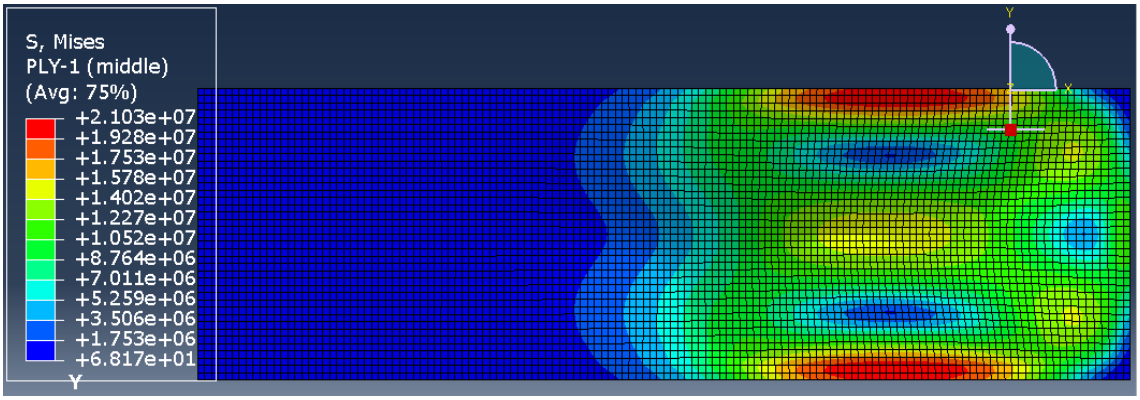

Figure 4-10: Ply-1 Von Mises Stress

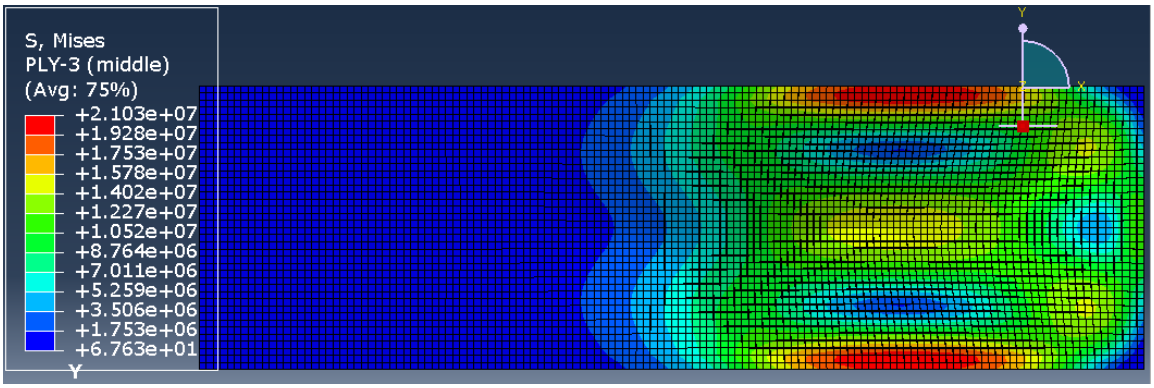

Figure 4-11: Ply-3 Von Mises Stress

Jute fiber-reinforced polyester ply (ply-2)

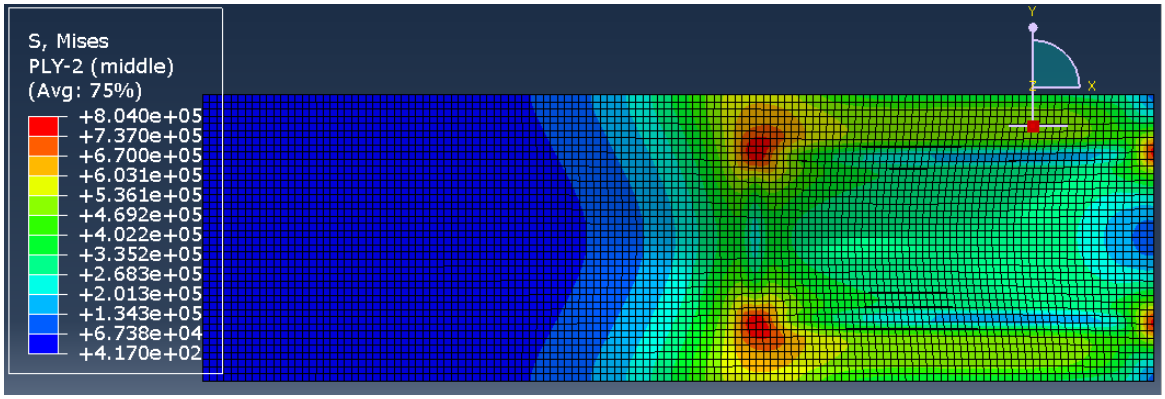

Figure 4-12: Ply-2 Von Mises Stress

The PET fiber-reinforced polyester plies show higher von Mises stress values compared to the jute fiber-reinforced ply. Specifically, ply-1 and ply-3, both PET-reinforced, exhibit similar von Mises stress values of 21.03 MPa, as shown in the figure above. In contrast, the jute fiber-reinforced ply

displays lower von Mises stress of 0.8040 MPa, as illustrated in Figure 4.12, indicating it undergoes less stress. This disparity in stress levels underscores an uneven distribution, with the PET fiber-reinforced plies bearing the majority of the load, while the jute fiber-reinforced ply contributes to damping and weight reduction.

2. Stress Components in each ply

This represents normal and shear stresses in various directions. For each ply of a composite laminate, the stress is analyzed within the local coordinate system of the ply, aligned with the material orientation. In a 2D plane stress state, the key stress components include longitudinal stress (S11), transverse stress (S22), and in-plane shear stress (S12). These are the primary stress results considered in such an analysis.

PET fiber-reinforced polyester ply (ply-1)

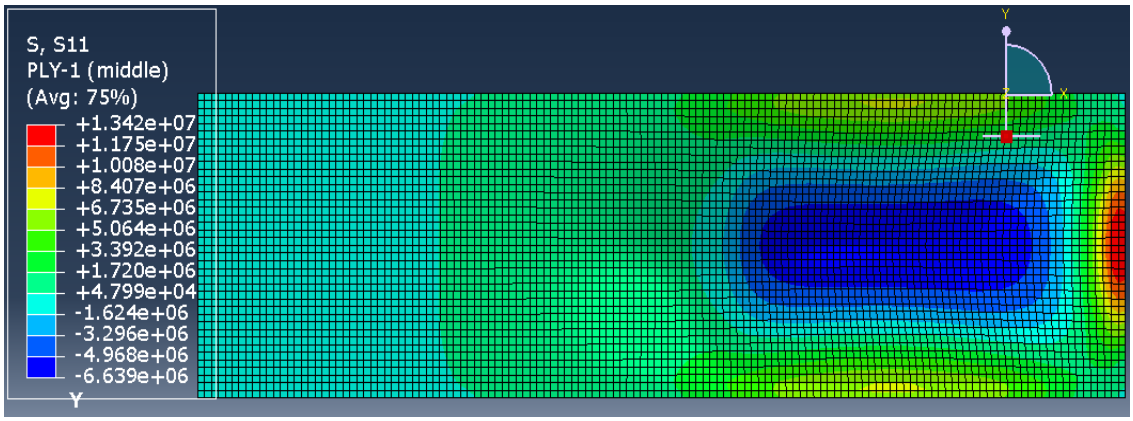

(a)

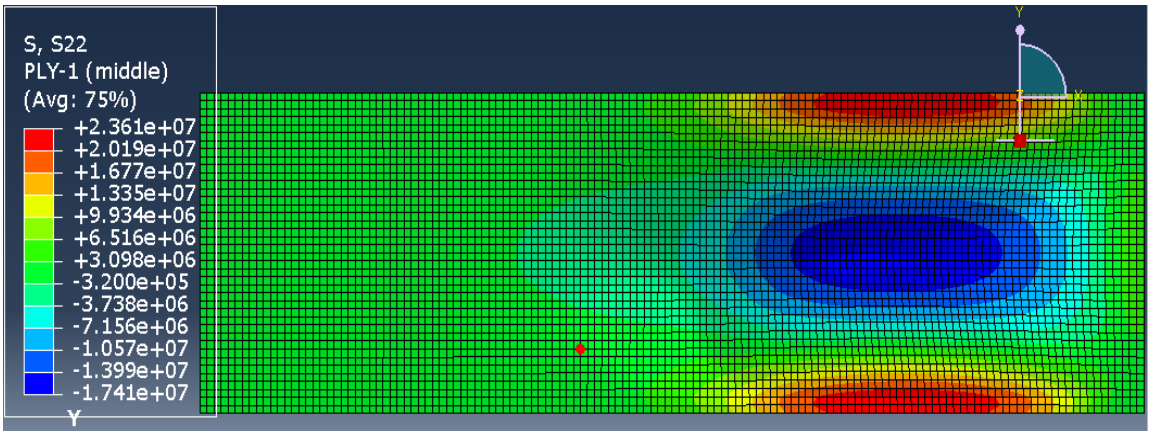

(b)

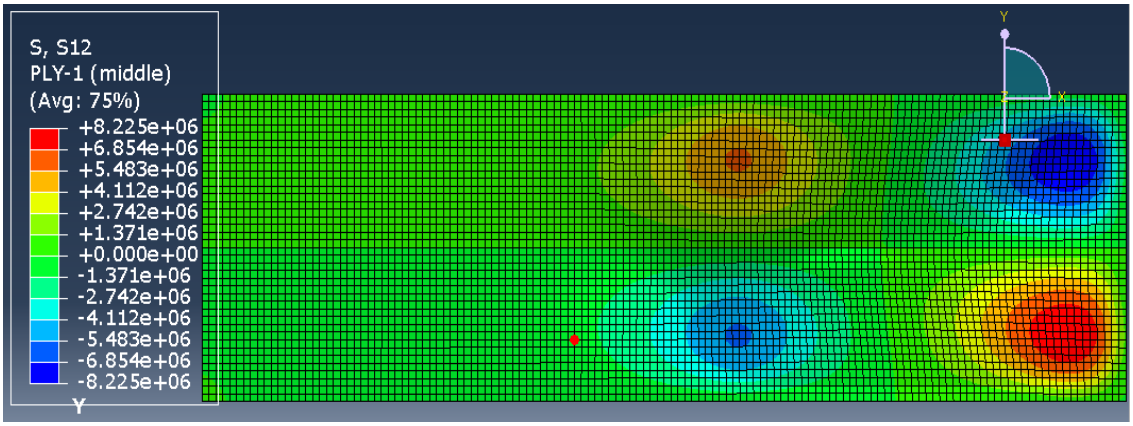

(c)

Figure 4-13: ply-1 stresses (a) Longitudinal(S11), (b) transverse(S22), and (c) in-plane shear(S12)

For the PET polyester lamina (ply-1), the longitudinal normal stress (S11) is less than the transverse normal stress (S22), attributed to the laminate's two 0° plies, which enhance stiffness in the transverse direction. FEA results reveal longitudinal tensile and compression strengths of 13.42MPa and 6.64MPa and transverse tensile and compression strengths of 23.61 MPa and 17.41 MPa, respectively, at the edges, while experimental values are higher at 67.5 MPa (transverse tensile) and 62.2 MPa (transverse compression). Also, The FEA-predicted shear strength (S12) is 8.22 MPa near the corners due to stress concentration, compared to the experimental shear strength of 25.5 MPa This indicates that the material, though stressed at the edges, remains within safe limits. The PET polyester layer (ply-1) functions securely within its strength boundaries, maintaining a safety factor of at least **2.855** against failure in transverse tensile strength for ply-1.

PET fiber-reinforced polyester ply (ply3)

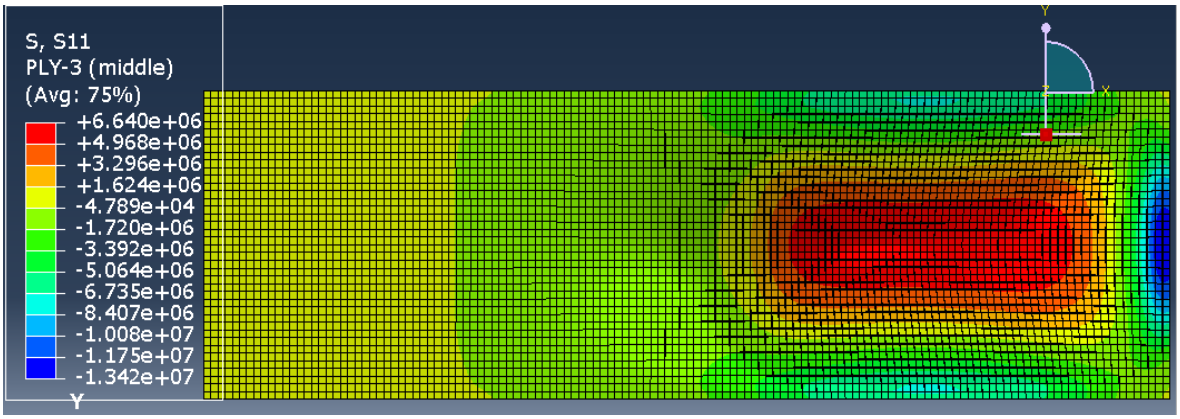

(a)

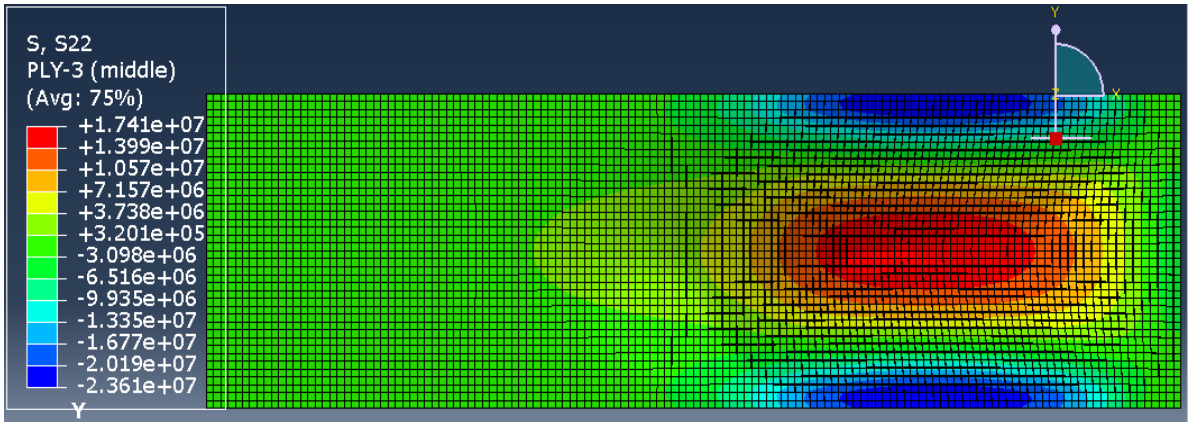

(b)

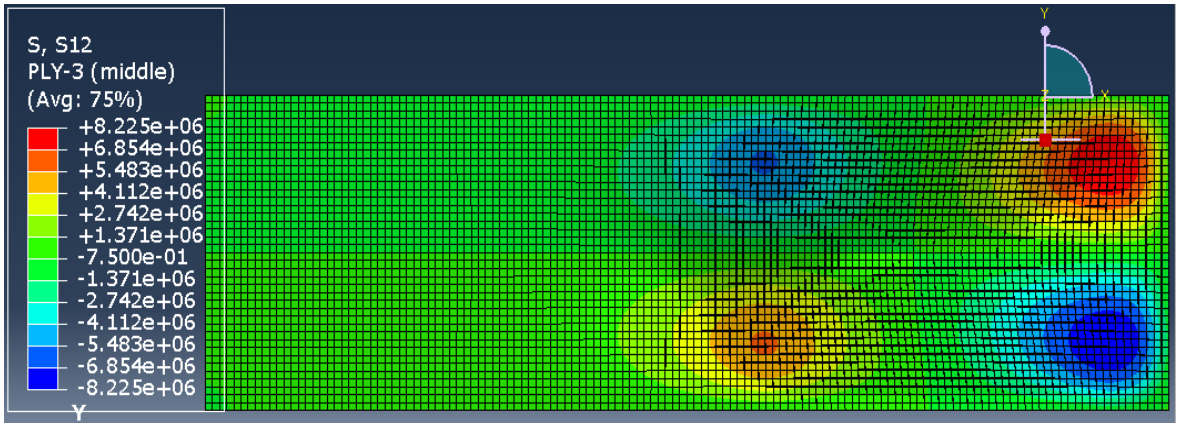

(c)

Figure 4-14: ply-3 stresses (a) Longitudinal(S11), (b) transverse(S22), and (c) in-plane shear(S12)

For the PET polyester lamina (ply-3), the longitudinal normal stress (S11), transverse normal stress (S22), and shear stress are very similar to those of ply-1, with values of (6.64 MPa and -13.42 MPa), (17.41 MPa and -23.61 MPa), and 8.22 MPa, respectively. The primary difference between ply-1 and ply-3 is the direction of the stress, while the stress magnitudes remain comparable. Experimental values, however, are higher at 67.5 MPa (transverse tensile) and 62.2 MPa (transverse compression). The PET polyester layer (ply-3) operates safely within its strength limits, with a minimum safety factor of **2.634** against failure in transverse compressive strength for ply-3.

Jute fiber-reinforced polyester ply (ply-2)

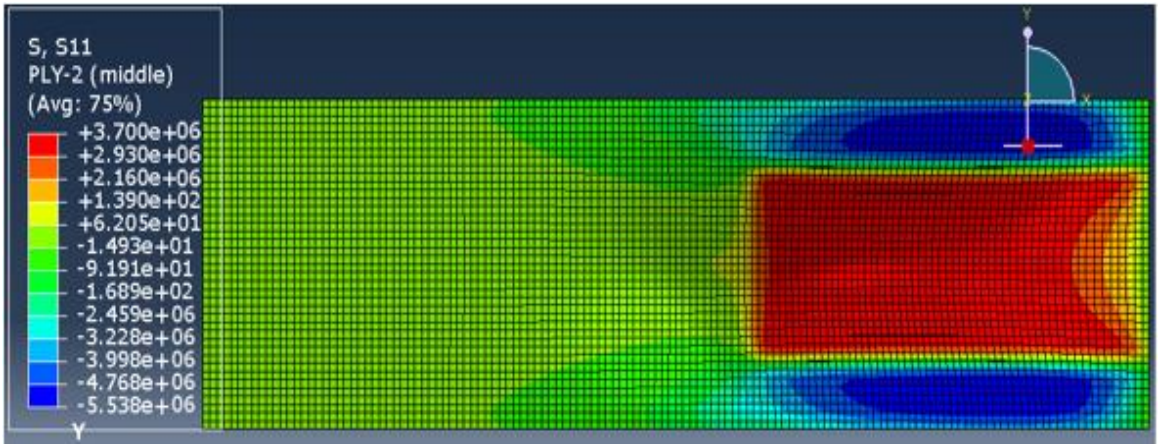

(a)

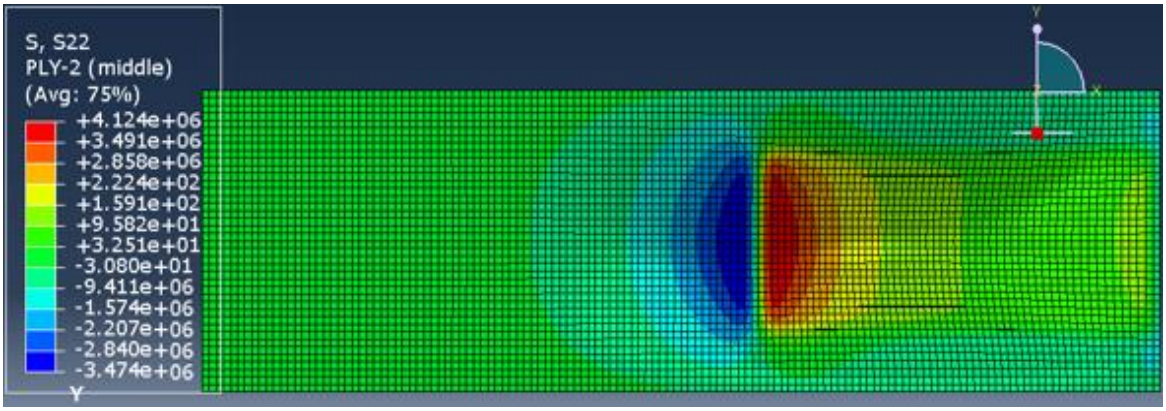

(b)

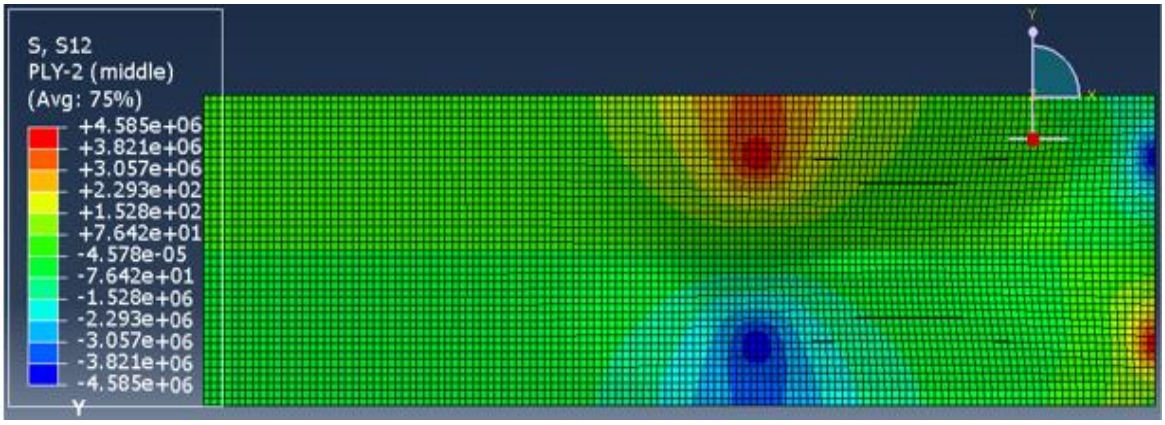

(c)

Figure 4-15: ply-2 stresses (a) Longitudinal(S11), (b) transverse(S22), and (c) in-plane shear(S12)

The jute polyester ply (ply-2) shows a maximum normal stress of 5.53 MPa in the fiber direction (S11) and a transverse stress of 4.12 MPa, both are lower than those in PET polyester fiber-

reinforced plies. Despite this, the jute ply maintains a reasonable load-bearing capacity, with a shear stress (S12) of 4.58 MPa. Experimental results, however, reveal much higher values: 69.4 MPa for longitudinal compression, 58.1 MPa for transverse tension, and 25.5 MPa for shear strength. FEA indicates that the stresses in the jute ply are well below its actual capacity, confirming that the ply is not overstressed. With a safety margin of 6.55 against failure, the jute-polyester lamina (ply-2) operates securely within its strength limits, ensuring a reliable and robust design.

3. Von Mises Stress on the hybrid composite plate

The Von Mises stress contour plot for the plate under a uniformly distributed payload is illustrated in Figure 4.16. The maximum Von Mises stress recorded is 23.04 MPa, which is localized in the region where the distributed load is applied (the loading box of the bus roof plate). This stress concentration arises from the focused application of force in that specific area, resulting in elevated stress levels.

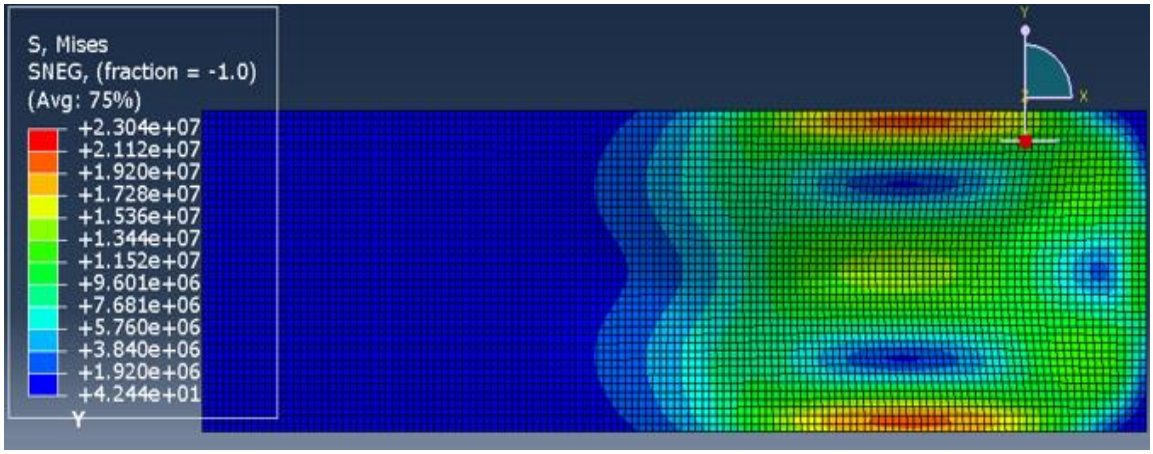

Figure 4-16: Contour plot of Von Mises Stress

4. Displacement (U, Magnitude)

The resulting displacement magnitude is shown in Figure 4.17, U=3.88mm representing the maximum deformation of the composite laminate under the applied load. This indicates the structure has low levels of deformation or it is very stiff.

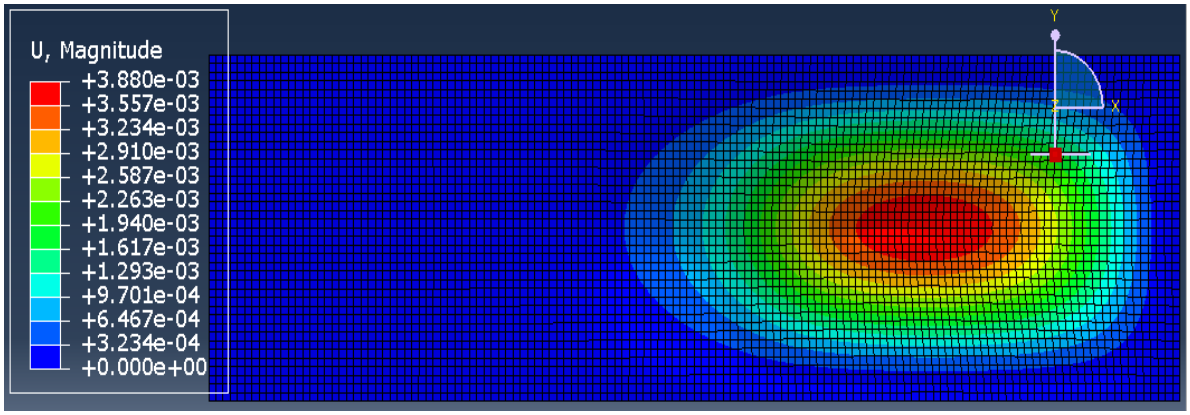

Figure 4-17: Deformation of hybrid composite plate

The maximum stress calculated by Optistruct was 21.14 MPa, whereas the finite element method (FEM) analysis conducted using Abaqus produced a result of 23.04 MPa, indicating an 8.9% difference. According to the Abaqus explicit model analysis, the maximum stress experienced by the developed hybrid jute/PET fiber composite structure was considerably lower than the experimentally measured tensile strength (107.4 MPa) and compressive strength (56.2 MPa) of the P-J-J-P hybrid composite with an identical layering sequence. This demonstrates that the bus roof plate functions within a safe operational range relative to its ultimate strength, with a minimum safety factor of **2.634** against failure in transverse compressive strength for ply-3. Furthermore, the maximum deflection (U-Magnitude) was 3.88 mm.

CHAPTER- FIVE

5. CONCLUSION AND RECOMMENDATION

5.1. Conclusion

This thesis focuses on the characterization, fabrication, and investigation of the mechanical and physical properties, design, and optimization of Jute/PET Hybrid Polymer Matrix Composite materials, specifically for lightweight vehicle components such as bus roof plates. The research methodology combined experimental testing, analytical modeling, and Finite Element Analysis (FEA) to derive meaningful insights. Based on these approaches, several key findings and conclusions have been established;

- The experimental results demonstrated that alkali treatment and fiber orientation significantly influence the tensile, compression, flexural, and impact properties. Alkaline treatment of jute fiber reduces moisture absorption while enhancing the mechanical properties of hybrid reinforced polyester composites.
- The TOPSIS method supports decision-making by evaluating various criteria and alternatives, enabling the identification of the optimal laminate composite stacking sequence for particular applications. Utilizing alkaline-treated jute fiber with PET fiber lamina as the outer layer (PET-J-J-PET) improved mechanical and physical properties.
- The optimized Jute/PET hybrid polyester composite bus roof for the modified ISUZU NPR71 4570cc buses resulted in a 34.58% reduction in weight compared to mild steel plate material, decreasing from 210.38 kg to 137.63 kg. Additionally, this modification could achieve a fuel saving of 0.2765 liters per 100 kilometers without affecting the vehicle's carrying capacity.
- Based on the HyperWorks (Optistruct) analysis, the optimized thickness results indicate that plies one and three, made of PET polyester, have a thickness of 1.2 mm, while ply two, composed of jute polyester, has a thickness of 4.8 mm. Using these thicknesses, Finite Element Analysis (FEA) conducted in Abaqus revealed that for the PET polyester lamina (ply-3), the longitudinal normal stress (S11), transverse normal stress (S22), and shear stress are very similar to those of ply-1, with values of (6.64

MPa and -13.42 MPa), (17.41 MPa and -23.61 MPa), and 8.22 MPa, respectively. The primary distinction between ply-1 and ply-3 lies in the direction of the stress, while the stress magnitudes remain comparable. Therefore, the PET-jute polyester composite laminate operates safely within its strength limits, demonstrating a safety factor of **2.634** against failure in transverse compressive strength for ply-3.

- The PET fiber layer primarily carries most of the load, whereas the jute fiber layer contributes lightweight characteristics and enhanced damping properties.
- Overall, the hybrid composite emerges as a promising alternative to steel for applications like bus roof plates, offering a balance between mechanical performance and weight reduction.

5.2. Recommendation

Based on the characterization and development of a hybrid composite plate for the bus roofs of modified ISUZU NPR71 4570cc buses in this thesis, it is recommended to replace metals and synthetic fibers with a hybrid composite combining natural and synthetic fibers with a matrix. This approach proved feasible for manufacturing internal and external vehicle parts, particularly the bus roof component studied here. Extending this replacement to most of the vehicle body could significantly reduce gross weight, enhancing overall efficiency and performance.

5.3. Future Work

Here are some recommendations for future research:

- In addition to the properties studied, further research can be conducted by considering different loading scenarios such as thermal load, and dynamic load effect on the composite.
- Additional research should be carried out to evaluate the composite's flammability, and machinability.
- Implement field trials of the composite material to gather empirical data on its performance under actual loading conditions.

REFERENCES

1. Prasad Yadav1, A.S.Y.G.P.P., *Review On Weight Reduction In Automobile.* January 2016. Vol.NO 4(ISSUE NO 01).
2. Chirinda, G.P. And S. Matope. *The Lighter The Better: Weight Reduction In The Automotive Industry And Its Impact On Fuel Consumption And Climate Change*. In *Proceedings Of The 2nd African International Conference On Industrial Engineering And Operations Management, Harare, Zimbabwe*. 2020.
3. Alliance, A., *Just How High-Tech Is The Automotive Industry?* 2014.
4. Olusegun, D.S., Et Al., *Assessing Mechanical Properties Of Natural Fibre Reinforced Composites For Engineering Applications.* 2012. 11(1): P. 780-784.
5. Ashik, K., Et Al., *A Review On Mechanical Properties Of Natural Fiber Reinforced Hybrid Polymer Composites.* 2015. 3(05): P. 420.
6. Pandey, P.D.A., *The Plastic Water Bottles – Impact On Environment.* JETIR, June 2023. Volume 10(Issue 6).
7. Obebe, S., A.J.I.J.O.E.A.S. Adamu, And Technology, *Plastic Pollution: Causes, Effects And Preventions.* 2020. 4(12): P. 85-95.
8. Thelma, C.C., L. Chitondo, And L. Ngulube, *Plastic Pollution: Causes, Effects, And Solutions.* International Journal Of Research Publication And Reviews, March 2024. Vol 5, No 3(ISSN 2582-7421).
9. Mohammed, S.A., G.I.J.S.-I.J.O.E.S. Al-Sarraj, And Applications, *Hybridization Influence On The Mechanical Properties Of Hybrid Composite Laminates: A Review.* 2024. 5(1): P. 64-70.
10. Panowicz, R., Et Al., *Properties Of Polyethylene Terephthalate (PET) After Thermo-Oxidative Aging.* 2021. 14(14): P. 3833.
11. Hu, X. And Z. Feng, *Advanced High-Strength Steel-Basics And Applications In The Automotive Industry*. 2021, Oak Ridge National Laboratory (ORNL), Oak Ridge, TN (United States).
12. Chehroudi, B., *Composite Materials And Their Uses In Cars Part II: Applications*. 2015, PhD Thesis.
13. Alves, C., Et Al., *Ecodesign Of Automotive Components Making Use Of Natural Jute Fiber Composites.* 2010. 18(4): P. 313-327.
14. Peças, P., Et Al., *Natural Fibre Composites And Their Applications: A Review.* 2018. 2(4): P. 66.
15. Kaw, A.K., *Mechanics Of Composite Materials*. 2005: CRC Press.
16. Barbero, E.J., *Introduction To Composite Materials Design*. 2010: CRC Press.

17. Hashim, M.K.R., Et Al., *The Effect Of Stacking Sequence And Ply Orientation On The Mechanical Properties Of Pineapple Leaf Fibre (Palf)/Carbon Hybrid Laminate Composites.* 2021. 13(3): P. 455.
18. Ashby, M.F. And D. Jones. *Engineering Materials 1. An Introduction To Their Properties And Applications*. In *Fuel And Energy Abstracts*. April 2021.
19. Sanjay, M.A., Et Al., *Studies On Mechanical Properties Of Jute/E-Glass Fiber Reinforced Epoxy Hybrid Composites.* 2016. 4(1): P. 15-25.
20. Hsissou, R., Et Al., *Polymer Composite Materials: A Comprehensive Review.* 2021. 262: P. 113640.
21. Rahman, M., Et Al., *Development Of Jute Hybrid Composites For Use In The Car Panels.* 2021. 7(3).
22. Yadav, S.P.S. And A.J.I.R.J.E.T. Verma, *Fabrication Of Composite Material Using Jute Fiber/Glass Fiber.* 2017. 4(8): P. 892-7.
23. Hassan, M., Et Al., *Characterization Of Jute And Glass Fiber Reinforced Polyester Based Hybrid Composite In This Research.* 2016. 51(2): P. 81-88.
24. Kaushik, P., J. Jaivir, And K.J.E.S.M. Mittal, *Analysis Of Mechanical Properties Of Jute Fiber Strengthened Epoxy/Polyester Composites.* 2017. 5(2): P. 103-112.
25. Prasad, L., Et Al., *Physical And Mechanical Behavior Of Hemp And Nettle Fiber-Reinforced Polyester Resin-Based Hybrid Composites.* 2022. 19(7): P. 2632-2647.
26. Prasad, L., Et Al., *Physical And Mechanical Behaviour Of Sugarcane Bagasse Fibre-Reinforced Epoxy Bio-Composites.* 2020. 13(23): P. 5387.
27. Prasad, L., Et Al., *Physical And Mechanical Properties Of Rambans (Agave) Fiber Reinforced With Polyester Composite Materials.* 2022. 19(13): P. 6104-6118.
28. Kumar, S.P. And S. Sharma, *Effect Of Alkali Treatment On Jute Fibre Composites*. 2007.
29. Kumar, A., A.J.I.E. Srivastava, And Management, *Preparation And Mechanical Properties Of Jute Fiber Reinforced Epoxy Composites.* 2017. 6(4): P. 1000234.
30. Ashraf, M.A., Et Al., *Jute Based Bio And Hybrid Composites And Their Applications.* 2019. 7(9): P. 77.
31. Rangasamy, G., Et Al., *An Extensive Analysis Of Mechanical, Thermal And Physical Properties Of Jute Fiber Composites With Different Fiber Orientations.* 2021. 28: P. 101612.
32. Biswas, S., Et Al., *Physical, Mechanical And Thermal Properties Of Jute And Bamboo Fiber Reinforced Unidirectional Epoxy Composites.* 2015. 105: P. 933-939.
33. Mishra, V., *Physical, Mechanical And Abrasive Wear Behaviour Of Jute Fiber Reinforced Polymer Composites*. 2014.
34. Ray, D., Et Al., *Effect Of Alkali Treated Jute Fibres On Composite Properties.* 2001. 24: P. 129-135.

35. Muthuvel, M., Et Al., *Characterization Study Of Jute And Glass Fiber Reinforced Hybrid Composite Material.* 2013. 2(4): P. 335-344.
36. Kumar, R. And A. Mohanty, *Structural Damping Properties Of Natural Porous Material Of Jute Felt.*
37. Fatima, S. And A.J.A.A. Mohanty, *Acoustical And Fire-Retardant Properties Of Jute Composite Materials.* 2011. 72(2-3): P. 108-114.
38. Ramesh, M., K. Palanikumar, And K.H.J.P.E. Reddy, *Comparative Evaluation On Properties Of Hybrid Glass Fiber-Sisal/Jute Reinforced Epoxy Composites.* 2013. 51: P. 745-750.
39. Farzana, M., Et Al., *Properties And Application Of Jute Fiber Reinforced Polymer-Based Composites.* 2022. 11(1): P. 084-094.
40. Melkamu, A., M.B. Kahsay, And A.G.J.J.O.N.F. Tesfay, *Mechanical And Water-Absorption Properties Of Sisal Fiber (Agave Sisalana)-Reinforced Polyester Composite.* 2019. 16(6): P. 877-885.
41. Mohammed, M., Et Al., *Challenges And Advancement In Water Absorption Of Natural Fiber-Reinforced Polymer Composites.* 2023. 124: P. 108083.
42. Sanjay, M. And B.J.M.T.P. Yogesha, *Studies On Natural/Glass Fiber Reinforced Polymer Hybrid Composites: An Evolution.* 2017. 4(2): P. 2739-2747.
43. Sever, K.J.J.O.R.P. And Composites, *The Improvement Of Mechanical Properties Of Jute Fiber/LDPE Composites By Fiber Surface Treatment.* 2010. 29(13): P. 1921-1929.
44. Shehu, U., Et Al., *Effects Of Naoh Modification On The Mechanical Properties Of Baobab Pod Fiber Reinforced LDPE Composites.* 2017. 36(1): P. 87-95.
45. Islam Bossunia, M., Et Al., *Γ–Irradiated Jute Reinforced Polypropylene Composites: Effect Of Mercerization And SEM Analysis.* 2016. 5(266): P. 2169-0022.10002.
46. Rodríguez, E.S. And A. Vázquez. *Alkali Treatment Of Jute Fabrics: Influence On The Processing Conditions And The Mechanical Properties Of Their Composites*. In *The 8th International Conference On Flow Processes In Composite Materials (FPCM8), Douai, France*. 2006.
47. Zannen, S., Et Al., *Effect Of Chemical Extraction On Physicochemical And Mechanical Properties Of Doum Palm Fibres.* 2014. 4(10): P. 203.
48. Wang, X., Et Al., *Effect Of Hot-Alkali Treatment On The Structure Composition Of Jute Fabrics And Mechanical Properties Of Laminated Composites.* 2019. 12(9): P. 1386.
49. Sinha, E. And S.J.B.O.M.S. Rout, *Influence Of Fibre-Surface Treatment On Structural, Thermal And Mechanical Properties Of Jute Fibre And Its Composite.* 2009. 32: P. 65-76.
50. Marsh, G.J.M.T., *Next Step For Automotive Materials.* 2003. 6(4): P. 36-43.
51. Prakash, S.J.I.R. And E. Journals, *Impact Of Plastic Pollution On Environment And Human Health: An Overview.* 2017. 1(5): P. 53-59.

52. Evode, N., Et Al., *Plastic Waste And Its Management Strategies For Environmental Sustainability*. 2021. 4: P. 100142.
53. Asgedom, A.G. And M.B.J.S.J.O.E.S. Desta, *The Environmental Impacts Of The Disposal Of Plastic Bags And Water Bottles In Tigray, Northern Ethiopia.* 2012. 2(1): P. 81-94.
54. Hussein, B.A., A.A. Tsegaye, And A.J.J.M.E.S. Abdulahi, *Assessment Of The Environmental And Health Impacts Of Disposal Plastics In Gode Town, Somali Regional State, Eastern Ethiopia.* 2021. 12(3): P. 455-471.
55. Balakrishnan, A., R.J.I.J.O.E.R. Flora, And Reviews, *The Environmental Impact Of Plastics And Recycling Of Plastic Waste.* 2017. 5(3): P. 14-20.
56. Forrest, M.J., *Recycling Of Polyethylene Terephthalate*. 2019: Walter De Gruyter Gmbh & Co KG.
57. Horvath, T., Et Al. *The Mechanical Properties Of Polyethylene-Terephthalate (PET) And Polylactic-Acid (PDLLA And PLLA), The Influence Of Material Structure On Forming*. In *IOP Conference Series: Materials Science And Engineering*. 2018. IOP Publishing.
58. Saidi, M.A.A., Et Al., *Thermal, Dynamic Mechanical Analysis And Mechanical Properties Of Polybutylene Terephthalate/Polyethylene Terephthalate Blends.* 2020. 82(5).
59. Hoque, M.A., Et Al., *Recycling Waste Polypropylene To Produce New Composite Materials With Jute Reinforcements.* 2023. 23(3): P. 21-32.
60. Sakthivel, S., Et Al., *Recycled Cotton/Polyester And Polypropylene Nonwoven Hybrid Composite Materials For Household Applications.* 2022. 113(1): P. 45-53.
61. Gudayu, A.D., Et Al., *Sisal Fiber Reinforced Polyethylene Terephthalate Composites; Fabrication, Characterization And Possible Application.* 2022. 30: P. 09673911221103317.
62. Stevens, C.V., *Industrial Applications Of Natural Fibres: Structure, Properties And Technical Applications*. 2010: John Wiley & Sons.
63. Yadav, Y.K., Et Al., *Natural Fiber Reinforced Rpet/Polyester Composites: A Review On Development, Mechanical Performance, And Sustainable Management.* 2023. 62(14): P. 1823-1843.
64. Huq, T., Et Al., *Fabrication And Characterization Of Jute Fiber-Reinforced PET Composite: Effect Of LLDPE Incorporation.* 2010. 49(4): P. 407-413.
65. Maslinda, A., Et Al., *Effect Of Water Absorption On The Mechanical Properties Of Hybrid Interwoven Cellulosic-Cellulosic Fibre Reinforced Epoxy Composites.* 2017. 167: P. 227-237.
66. Gadisa, D.G., A.G.J.I.J.F.S. Tesfay, And M.D. Optimization, *Developing An Alternative Crossbar Material From Jute/E-Glass Fiber Hybrid Reinforced Polymer Matrix Composite.* 2024. 15: P. 1.

67. Pandita, S.D., Et Al., *Evaluation Of Jute/Glass Hybrid Composite Sandwich: Water Resistance, Impact Properties And Life Cycle Assessment.* 2014. 33(1): P. 14-25.
68. Zhao, D., Et Al., *Flexural Behavior Evaluation Of Needle-Punched Glass/Jute Hybrid Mat Reinforced Polymer Composites.* 2017. 200: P. 10-17.
69. Raja, T., Et Al., *Evaluation Of Mechanical Properties Of Natural Fibre Reinforced Composites: A Review.* 2017. 8(7): P. 915-924.
70. Yahaya, R., Et Al., *Effect Of Layering Sequence And Chemical Treatment On The Mechanical Properties Of Woven Kenaf–Aramid Hybrid Laminated Composites.* 2015. 67: P. 173-179.
71. Sabaei, D., J. Erkoyuncu, And R.J.P.C. Roy, *A Review Of Multi-Criteria Decision Making Methods For Enhanced Maintenance Delivery.* 2015. 37: P. 30-35.
72. Daniel, D.J., K.J.S.R. Panneerselvam, And Letters, *Process Parameters Optimization For Friction Vibration Joining Of Polypropylene/Spheri Glass Composites Using TOPSIS.* 2020. 27(06): P. 1950167.
73. Velasquez, M. And P.T. Hester. *An Analysis Of Multi-Criteria Decision-Making Methods*. 2013.
74. Mohammadi, A., Et Al., *Introducing A New Method To Expand TOPSIS Decision Making Model To Fuzzy TOPSIS.* 2011. 2(1): P. 150-159.
75. Swain, P.T.R., S.J.A.M. Biswas, And Materials, *Selection Of Materials Using Multi-Criteria Decision Making Method By Considering Physical And Mechanical Properties Of Jute/Al2O3 Composites.* 2014. 592: P. 729-733.
76. TODOR, M.-P., C. Bulei, And I.J.A.O.T.F.O.E.H.-I.J.O.E. Kiss, *An Overview On Fiber-Reinforced Composites Used In The Automotive Industry.* 2017. 15(2).
77. Bushi, L.J.A.A., *EDAG Silverado Body Lightweighting Final LCA Report.* 2018.
78. Knittel, C.R.J.J.O.E.P., *Reducing Petroleum Consumption From Transportation.* 2012. 26(1): P. 93-118.
79. Kavrakov, I., *Structural Optimization Of Composite Cross-Sections And Elements Using Energy Methods.* 2014.
80. NANDI, A.K. And H.J.J. MISHRA, *Stress Calculation For Rectangular Plate Using Simplified Analytical Method.* 2017. 3(04): P. 174-178.
81. Imrak, C. And I.J.A.M.S. Gerdemeli, *An Exact Solution For The Deflection Of A Clamped Rectangular Plate Under Uniform Load.* 2007. 1(43): P. 2129-2137.
82. D.Purushottam Reddy1, S.S.A., D.Srikanth3, JV.Mohanachari4, *DESIGN AND ANALYSIS OF BUS BODY SUPERSTRUCTURE.* IJRDO-Journal Of Mechanical And Civil Engineering ISSN: 2456-1479, February 2016 Volume-2 (Issue-2).
83. Olason, A. And D. Tidman, *Methodology For Topology And Shpe Optimization In The Design Process.* 2010.

84. Inc., A.E., *Introduction To Practical Aspects Of Composites With Altair Optistruct. 2019. [Online].* Available: Https://Www.Altair.Com/Radioss/.
85. Suleiman, O.M.A.E., *Mechanical Properties Of Composite Laminated Plates.* Int. J. Adv. Sci. Res. Eng., 2017. Vol. 02, (No. Issue 09).
86. Öztekin, H.F., Et Al., *Effect Of Fiber Type And Thickness On Mechanical Behavior Of Thermoplastic Composite Plates Reinforced With Fabric Plies.* Journal Of Structural Engineering & Applied Mechanics, 2022. 5(3): P. 161-169.
87. O. Atteaa Al-Hassany, M., Et Al., *Effect Of Fiberglass Form On The Tensile And Bending Characteristic Of Epoxy Composite Material.* AIMS Materials Science, 2020. 7(5): P. 583-595.
88. Gadisa, D.G. And A.G. Tesfay, *Developing An Alternative Crossbar Material From Jute/E-Glass Fiber Hybrid Reinforced Polymer Matrix Composite.* International Journal For Simulation And Multidisciplinary Design Optimization, 2024. 15.
89. Manual, R.R.L.A.U.G.A.P., *Polyester Resin User Guide And Manual.* Resin Libr., May 2021. Vol. Version 1(No. May 2021, .): P. Pp. 1–6, 2021.
90. Nouryon, *Butanox ® M-50 Product Description Methyl Ethyl Ketone Peroxide, Solution In Dimethyl Phthalate.* [Online]. Available: Www.Akzonobel.Com/Polymer, 2008: P. Pp. 1–3,.
91. Tesfay, A.G., M.B. Kahsay, And P.S.J.J.O.N.F. Kumar, *Effects Of Chemical Treatment, Hybridization, And Hybrid Fiber Stacking Sequence And Orientation On Tensile And Impact Strength Of Continuous Sisal Fiber Reinforced Polyester Composites.* 2022. 19(7): P. 2619-2631.
92. Parker, E.E., E.J.I. Moffett, And E. Chemistry, *Physical Properties Of Polyester Resin.* 1954. 46(8): P. 1615-1618.
93. Schwaegerle, P.R.J.J.O.V.T., *Measuring The Bulk Flow Properties Of PVC Resins.* 1983. 5(3): P. 86-90.
94. Saba, N., Et Al., *An Overview Of Mechanical And Physical Testing Of Composite Materials.* 2019: P. 1-12.
95. D570, A. *Standard Test Method For Water Absorption Of Plastics.* Reapproved 2010. American Society For Testing And Materials.
96. ASTM, *Astm D3039/D3039M.* Annu. B. ASTM Stand., 2014: P. Pp. 1–13,.
97. ASTM, *D6641: Standard Test Method For Compressive Properties Of Polymer Matrix Composite Materials Using A Combined Loading Compression (CLC) Test Fixture,.* Annu. B. Astm Stand., 2014. Vol. 01(Doi: 10.1520/D6641.): P. Pp. 1–13.
98. ASTM, *ASTM D 7264/D 7264M-07 Standard Test Method For Flexural Properties Of Polymer Matrix Composite Material,* Annu. B. ASTM Stand., 2018.

99. ASTM, *ASTM D 256 Standard Test Methods For Determining The Izod Pendulum Impact Resistance Of Plastics,* Annu. B. ASTM Stand., 2018.
100. Https://Isuzu-Ethiopia.Com. *Spec Sheet*.
101. Mittelstedt, C., *Theory Of Plates And Shells*. 2023: Springer.
102. Hashin, Z., *Fiber Composite Analysis And Design: Composite Materials And Laminates, Volume I*. 1997.
103. "Https://Www.Structx.Com/Plates.Html.".
104. Panchal, B.J.D.S.C.O.E.M., India, *Classical Laminate Theory (CLT) And Its Use For Designing And Manufacturing Of FRP Plates.* 2021.

APPENDIX-A

RULE OF MIXTURE

- Fiber and matrix weight fraction (W_F, W_M)

$$Fiber\ weight\ fraction\ = \frac{Weight\ of\ Fiber}{Total\ weight\ of\ the\ composite}$$

$$Fiber\ weight\ fraction\ = \frac{Weight\ of\ Fiber}{Total\ weight\ of\ the\ composite}$$

$$Total\ weight\ of\ composite\ =\ the\ sum\ of\ fiber\ and\ matrix\ weight$$

- Fiber and matrix volume fraction (V_F, V_M)

$$Volume\ of\ fibers = \frac{Weight\ of\ fiber}{Density\ of\ fiber}$$

$$Volume\ of\ matrix = \frac{Weight\ of\ matrix}{Density\ of\ matrix}$$

$$Total\ Volume\ of\ composite\ =\ sum\ of\ Volume\ of\ fibers + Volume\ of\ matrix$$

$$Volume\ fraction\ of\ Fiber\ = \frac{Volume\ of\ fibers}{Total\ Volume\ of\ composite}$$

$$Volume\ fraction\ of\ Matrix\ = \frac{Volume\ of\ matrix}{Total\ Volume\ of\ the\ composite}$$

Table A - 1: The experimental and theoretical densities of composite laminate results summary

Stacking Sequence	molded weight (kg)	ρtheo=1/[wf/ρf + wm/ρm] (g/cm^3)	ρexp (molded mass/volume)
P-J-J-P	0.377	1.298304	1.0250
J-P-P-J	0.367	1.298065	1.0190
P-J-J-P	0.357	1.297970	1.0011
P-J-P-J	0.364	1.297987	1.0182
PET Polyster	0.132	1.288167	1.3054

Table A - 2: Composite laminas property

Variables	PET polyester lamina	Jute polyester lamina
E1 (GPa)	2.533971	7.438216
E2 (GPa)	4.013705	4.939528
V12	0.291182	0.275653
V21	0.46122	0.183054
G12(GPa)= G13	2.792269	4.404167
Q11(GPa)	2.927074	7.833488
Q22(GPa)	4.636364	5.202018
Q12(GPa)	1.350026	1.433951
G23(GPa)	1.394755	1.35990

Table A - 3: Average Water absorption test results

Water absorption rate (%)						
Laminates	24 hrs	48 hrs	72 hrs	96 hrs	120 hrs	144 hrs
P-J-J-P (UJF)	1.38	1.77	1.89	1.97	2.09	2.13
J-P-P-J	2.81	2.99	3.03	3.08	3.11	3.13
P-J-J-P	0.65	0.99	1.03	1.05	1.09	1.13
P-J-P-J	0.95	1.28	1.46	1.59	1.75	1.76
PET polyster	0	0	0.01	0.01	0.15	0.15

Table A - 4: Average mechanical property Test results

Laminates	Tensile strength (MPa)	Compressive strength (MPa)	Flexural strength (MPa)	Impact strength (KJ/m2)
P-J-J-P (UJF)	83.78	49.1	183.6	79.8
J-P-P-J	77.3	38.3	128.7	71.3
P-J-J-P	107.4	56.2	191.2	81.3
P-J-P-J	91.6	52.2	187.9	74.6
PET polyster	48.4	26.4	97.8	45.5

APPENDIX-B

TOPSIS Analysis steps

TOPSIS method involves number of steps;

Step 1: Establishing a decision matrix for ranking consisting of alternatives and criterias.

Samples	Tensile Strength (Mpa)	Compression Strength (Mpa)	Flexural Strength (Mpa)	Impact Strength (Mpa)	Water Absorption (%)	density (g/cm)
P-J-J-P (UJF)	83.78	49.1	183.6	79.8	2.13	1.298
J-P-P-J	77.3	38.3	128.7	71.3	3.13	1.298
P-J-J-P	107.4	56.2	191.2	81.3	1.13	1.2978
P-J-P-J	91.6	52.2	187.9	74.6	1.76	1.298
PET polyster	48.4	26.4	97.8	45.5	0.15	1.288

Step 2: Construct the normalized decision matrix;

$$\bar{X}_{ij} = \frac{X_{IJ}}{\sqrt{\sum_{i=1}^{m} X_{ij}^2}}$$

Relative importance weighting

Importance	5	4	3	2	1
Description	Most important	More important	Moderate important	Less important	Not-important
Difference b/n the alternatives	Significant variable	Comparable variable	Almost equally	equally	Equally
Weighting	0.2	0.15	0.1	0.5	0

Criteria →	Tensile Strength	Compression Strength	Flexural Strength	Impact Strength	Water Absorption	Density
Importance in the application	4	4	4	5	3	3
Weight =1	0.15	0.15	0.15	0.2	0.1	0.1

Normalization						
Samples	Tensile ST	Compression ST	Flexural ST	Impact ST	Water abs	Density
P-J-J-P (UJF)	0.4462	0.4801	0.5059	0.4978	0.4922	0.4479
J-P-P-J	0.4116	0.3745	0.3546	0.4448	0.7232	0.4479
P-J-J-P	0.5719	0.5496	0.5269	0.5072	0.2611	0.4478
P-J-P-J	0.4878	0.5104	0.5178	0.4654	0.4067	0.4479
PET polyster	0.2577	0.2582	0.2695	0.2838	0.0347	0.4445

Step 3: Determine the weighted normalized decision matrix;

$$V_{ij} = \bar{X}_{ij}\, x\, W_j$$

weighted normalized						
Samples	Tensile strength	Compression strength	Flexural strength	Impact strength	Water abs	Density
P-J-J-P (UJF)	0.066923	0.072019	0.075887	0.099561	0.049215	0.044791
J-P-P-J	0.061746	0.056178	0.053195	0.088956	0.072321	0.044791
P-J-J-P	0.085790	0.082433	0.079028	0.101433	0.026109	0.044784
P-J-P-J	0.073169	0.076566	0.077664	0.093074	0.040666	0.044791
PET polyster	0.038661	0.038723	0.040423	0.056767	0.003465	0.044446

Step 4: Calculate the positive (best) ideal solutions (V+) and negative (worst) ideal solutions (V-) for each criterion from the alternatives.

Ideal solution	Tensile Strength	Compression Strength	Flexural Strength	Impact Strength	Water Absorption	Density
V+	0.0857907	0.0824336	0.0790285	0.1014333	0.0034659	0.0444464
V-	0.0386617	0.0387232	0.0404236	0.0567677	0.0723213	0.0447915

Step 5: Calculate the Euclidean distance between the target alternative and the best/worst alternative Si+/Si- separation measure value using the Euclidean distance method;

$$S_i^+ = \left[\sum_{i=1}^{m}\left(V_{ij} - V_i^+\right)^2\right]^{0.5}$$

And

$$S_i^- = \left[\sum_{i=1}^{m}\left(V_{ij} - V_i^+\right)^2\right]^{0.5}$$

Where i = 1, 2, 3…m

	Distance separation	
Samples	S_i^+	S_i^-
P-J-J-P (UJF)	0.050704	0.074366
J-P-P-J	0.082653	0.045132
P-J-J-P	0.022646	0.098755
P-J-P-J	0.040613	0.079561
PET polyster	0.087276	0.068856

Step 6: Determine the relative closeness to the ideal solution for each alternative.

Step 7: Finally Rank the preference order.

To calculate the performance score, P_i ; $P_i = \frac{S_i^-}{S_i^+ + S_i^-}$

Sample	**Performance score**	**Rank**
P-J-J-P (UJF)	0.59459	3
J-P-P-J	0.35318	5
P-J-J-P	**0.81346**	**1**
P-J-P-J	0.66204	2
PET polyster	0.44101	4

APPENDIX-C

Classical Laminate Theory Calculation (CLT)

- The value of the reduced stiffness matrix [Qij] for each ply is using Eqn(3.22)

The stiffness matrix for ply one and ply four lamina of PET polyester lamina

$$[Q]_{PET} = \begin{bmatrix} 2.927 & 1.350 & 0 \\ 1.350 & 4.636 & 0 \\ 0 & 0 & 2.792 \end{bmatrix} Gpa \ \ and$$

The stiffness matrix for ply two and ply three lamina of jute polyester lamina

$$[Q]_J = \begin{bmatrix} 7.833 & 1.434 & 0 \\ 1.434 & 5.202 & 0 \\ 0 & 0 & 4.404 \end{bmatrix} Gpa \ \ and$$

- The laminate extensional stiffness matrix is calculated by using the stiffness matrixes and thickness of the lamina using Equation (3.28-3.30)

$$[\mathrm{A}] = \sum_{\mathrm{k}=1}^{4} \left[\overline{\mathrm{Q}}_{\mathrm{ij}}\right]_{\mathrm{k}} \left(\mathrm{Z_k} - \mathrm{Z_{k-1}}\right) = \begin{bmatrix} 10.76 \times 10^6 & 2.784 \times 10^6 & 0 \\ 2.784 \times 10^6 & 9.838 \times 10^6 & 0 \\ 0 & 0 & 3.598 \times 10^6 \end{bmatrix} pa.m$$

$$[\mathrm{B}] = \frac{1}{2}\sum_{\mathrm{k}=1}^{4}\left[\overline{\mathrm{Q}}_{\mathrm{ij}}\right]_{\mathrm{k}} \left(\mathrm{Z_k}^2 - \mathrm{Z_{k-1}}^2\right) = 0$$

$$[\mathrm{D}] = \frac{1}{3}\sum_{\mathrm{k}=1}^{4}\left[\overline{\mathrm{Q}}_{\mathrm{ij}}\right]_{\mathrm{k}} \left(\mathrm{Z_k}^3 - \mathrm{Z_{k-1}}^3\right) = \begin{bmatrix} 2.36 & 0.907 & 0 \\ 0.907 & 3.137 & 0 \\ 0 & 0 & 1.9956 \end{bmatrix} pa.m^3$$

- Calculating mid-plane strains

$$\begin{Bmatrix} N_X \\ N_Y \\ N_{XY} \end{Bmatrix} = \begin{bmatrix} A_{11} & A_{12} & A_{16} \\ A_{12} & A_{22} & A_{26} \\ A_{16} & A_{26} & A_{66} \end{bmatrix} \begin{Bmatrix} \varepsilon_X^0 \\ \varepsilon_Y^0 \\ \gamma_{XY}^0 \end{Bmatrix}$$

$$\begin{Bmatrix} \varepsilon_X^0 \\ \varepsilon_Y^0 \\ \gamma_{XY}^0 \end{Bmatrix} = \begin{bmatrix} 1.0028 & -0.284 & 0 \\ -0.284 & 1.0967 & 0 \\ 0 & 0 & 2.779 \end{bmatrix} \times 10^{-7} \begin{Bmatrix} 4496.25 \\ 1926.96 \\ 0 \end{Bmatrix} = \begin{bmatrix} 396.158 \times 10^{-7} \\ 83.6362 \times 10^{-7} \\ 0 \end{bmatrix}$$

$$\begin{Bmatrix} M_X \\ M_Y \\ M_{XY} \end{Bmatrix} = \begin{bmatrix} D_{11} & D_{12} & D_{16} \\ D_{12} & D_{22} & D_{26} \\ D_{16} & D_{26} & D_{66} \end{bmatrix} \begin{Bmatrix} K_X \\ K_Y \\ K_{XY} \end{Bmatrix}$$

$$\begin{Bmatrix} K_X \\ K_Y \\ K_{XY} \end{Bmatrix} = \begin{bmatrix} 0.4767 & -0.13782 & 0 \\ -0.13782 & 0.35862 & 0 \\ 0 & 0 & 0.501 \end{bmatrix} \begin{Bmatrix} -211.5 \\ -52.87 \\ 0 \end{Bmatrix} = \begin{bmatrix} -93.535 \\ 10.1886 \\ 0 \end{bmatrix} /m$$

- Calculating global strains of the plies

$$\begin{Bmatrix} \varepsilon_X \\ \varepsilon_Y \\ \gamma_{XY} \end{Bmatrix} = \begin{Bmatrix} \varepsilon_X^0 \\ \varepsilon_Y^0 \\ \gamma_{XY}^0 \end{Bmatrix} + z \begin{Bmatrix} K_X \\ K_Y \\ K_{XY} \end{Bmatrix} = \begin{Bmatrix} -0.1870 \\ 0.020 \\ 0 \end{Bmatrix}$$

- Calculating local stress and strains of each lamina

A transformation matrix

$$[T] = \begin{bmatrix} \mathrm{m}^2 & \mathrm{n}^2 & 2\mathrm{mn} \\ \mathrm{n}^2 & \mathrm{m}^2 & -2\mathrm{mn} \\ -\mathrm{mn} & \mathrm{mn} & \mathrm{m}-\mathrm{n}^2 \end{bmatrix} = \begin{bmatrix} 1 & 0 & 0 \\ 0 & 1 & 0 \\ 0 & 0 & 1 \end{bmatrix}, \text{Where; } \mathrm{m} = \cos\theta \text{ and } \mathrm{n} = \sin\theta$$

Local strains

$$\begin{bmatrix} \varepsilon_1 \\ \varepsilon_2 \\ \gamma_{12/2} \end{bmatrix} = [T] \begin{bmatrix} \varepsilon_X \\ \varepsilon_Y \\ \gamma_{XY/2} \end{bmatrix} = \begin{bmatrix} 1 & 0 & 0 \\ 0 & 1 & 0 \\ 0 & 0 & 1 \end{bmatrix} \begin{bmatrix} \varepsilon_X \\ \varepsilon_Y \\ \gamma_{XY/2} \end{bmatrix} = \begin{bmatrix} -0.187 \\ 0.020 \\ 0 \end{bmatrix}$$

Tsai-Wu Failure Theory Components

$$g(u) = F_1\sigma_1 + F_2\sigma_2 + F_6\sigma_{12} + F_{11}{\sigma_1}^2 + F_{22}{\sigma_2}^2 + F_{66}{\sigma_{12}}^2 + F_{12}\sigma_1\sigma_2 \leq 1$$

$$F_1 = \frac{1}{X_t} - \frac{1}{X_c},\ F_2 = \frac{1}{Y_t} - \frac{1}{Y_c}$$

$$F_6 = 0$$

$$F_{11} = \frac{1}{X_t X_c},\ F_{22} = \frac{1}{Y_t Y_c}$$

$$F_{66} = \frac{1}{(\tau_{12})^2_{Ult}}, F_{12} = -\frac{1}{2}\sqrt{\frac{1}{X_t X_c Y_t Y_c}}$$

Table C - 1: Strength property of each lamina

Strengths	PET polyester lamina	Jute polyester lamina
Longitudinal strength in tension, X_t	72.5Mpa	89.5MPa
Longitudinal strength in compression, X_c	-65.5Mpa	-69.4MPa
Transverse strength in tension, Y_t	67.5Mpa	58.1MPa
Transverse strength in compression, Y_c	-62.2Mpa	-67.3MPa
Shear strength, S	25.5Mpa	30MPa

Strength Ratio

$$SR = \frac{Ultimate\ stress}{Applied\ stress} > 1$$

APPENDIX-D

HYPER WORK-OPTISTRUCT

Optistruct Optimization Input File

```
$$
$$ Optistruct Input Deck Generated by HyperMesh Version : 2019.1.0.20
$$ Generated using HyperMesh-Optistruct Template Version : 2019.1.0.20
$$
$$   Template:  optistruct
$$
$$ optistruct
$
OUTPUT,FSTOSZ,        ,4
CFAILURE(NDIV=1) = ALL
CSTRAIN(NDIV=1) = YES
CSTRESS(NDIV=1) = ALL
DISPLACEMENT = ALL
$$--------------------------------------------------------------------------$
$$                    Case Control Cards                                  $
$$--------------------------------------------------------------------------$
$$
$$  OBJECTIVES Data
$
$HMNAME OBJECTIVES       1objective
$
DESOBJ(MIN)=1
$
$
$HMNAME LOADSTEP              1"LS"       1
$
SUBCASE       1
  LABEL LS
ANALYSIS STATICS
  SPC =        1
  LOAD =       2
  DESSUB =      2
$$-------------------------------------------------------------
$$ HYPERMESH TAGS
$$-------------------------------------------------------------
$$BEGIN TAGS
$$END TAGS
$
BEGIN BULK
```

```
$
$HMNAME PLYS                1"ply1"
$HWCOLOR PLYS               1      23
PLY     1       1       0.0005 0.0     YES
+       1
$
$HMNAME PLYS                2"ply2"
$HWCOLOR PLYS               2      52
PLY     2       2       0.001  90.0    YES
+       2
$
$HMNAME PLYS                3"ply3"
$HWCOLOR PLYS               3      23
PLY     3       1       0.0005 0.0     YES
+       3
$$
$$  Stacking Information for Ply-Based Composite Definition
$$
$HMNAME LAMINATES           1"laminate1"
$HWCOLOR LAMINATES          1       5
STACK   1           1       2       3
$$
$HMSET       1       2 "ply1"
$HMSETTYPE       1 "formula"
SET     1       ELEM    LIST
+       1       THRU  1340
$
$HMSET       2       2 "ply2"
$HMSETTYPE       2 "formula"
SET     2       ELEM    LIST
+       1       THRU  1340
$
$HMSET       3       2 "ply3"
$HMSETTYPE       3 "formula"
SET     3       ELEM    LIST
+       1       THRU  1340
$
$HMNAME OPTICONTROLS       1"optistruct_opticontrol" 1
$
DOPTPRM DESMAX  200

$HMNAME DESVARS        1thickness
DSIZE   1       STACK   1
+       MEMBSIZ 0.015
```

```
+       COMP    LAMTHK  0.0005 0.002
+       COMP    BALANCE 45.0    -45.0           BYANG
$$
$$  OPTIRESPONSES Data
$$
DRESP1  1       MASS    MASS                1
DRESP1  2       FI INDEXCFAILUREPCOMP       1    TSAI     ALL       1
$$
$$  OPTICONSTRAINTS Data
$$
$HMNAME OPTICONSTRAINTS       1MAX FI
$
DCONSTR       1       2       0.99

DCONADD       2       1
```